Escola Politècnica Superior de Castelldefels
UNIVERSITAT POLITÈCNICA DE CATALUNYA

TREBALL DE FI DE CARRERA

TÍTOL DEL TFC: Production and Characterization of Mechanical Properties of Metallic Glasses

TITULACIÓ: Enginyeria Tècnica Aeronàutica, especialitat Aeronavegació

AUTOR: Oscar Belart Bayo

DIRECTOR: Jorge Serrano Gutiérrez

DATA: 18 març de 2009

Títol: Producció i caracterització de propietats mecàniques de vidres metàl·lics

Autor: Oscar Belart Bayo

Director: Jorge Serrano Gutiérrez

Data: 18 de març de 2009

Resum

Els vidres metàl·lics representen un nou tipus de material. Van ser descoberts el 1960 i tenen unes propietats estructurals i mecàniques molt interessants que els han fet idonis per aplicacions en molts camps. Han estat utilitzats des d'algunes dècades degut a les seves propietats magnètiques i ara les mecàniques atrauen l'atenció de la comunitat científica.

L'objectiu d'aquest treball és produir i caracteritzar el vidre metàl·lic $Pd_{77}Si_{16.5}Cu_{6.5}$ utilitzant diferents tècniques. Per a la producció es van utilitzar un Arc-Melter, un aparell per a fondre elements en boles mitjançant arcs voltaics, i un Melt-Spinner, una màquina de refredament ràpid que produeix cintes amb espessors micromètrics. Per tal de comprovar la validesa de les mostres, aquestes es van analitzar amb la tècnica Scanning Electron Microscopy (SEM), la qual és capaç d'extreure'n la composició real amb un error molt reduït. Per a la caracterització es va utilitzar l'Inelastic Neutron Scattering (INS) per tal de descobrir algunes de les seves propietats vibracionals.

També es caracteritza un segon aliatge prefabricat, $Ce_{70}Al_{10}Ni_{10}Cu_{10}$, amb la tècnica Dynamic Mechanical Analysis (DMA) la qual ens donà informació sobre les seves propietats mecàniques. Es van trobar dos paràmetres fonamentals: la temperatura de transició vítria i la fragilitat del material.

El treball conté dues parts bàsiques: producció i caracterització on s'explica cada mètode mencionat anteriorment i els resultats obtinguts, a més a més de les conclusions pertinents de cada apartat.

Finalment, les conclusions del treball a mode de resum de dates i propostes per tal de continuar amb la investigació d'aquests materials.

Title: Production and Characterization of Mechanical Properties of Metallic Glasses

Author: Oscar Belart Bayo

Director: Jorge Serrano Gutiérrez

Date: March, 18th 2008

Overview

The metallic glasses represent a new class of materials. They were discovered in 1960 and they have interesting structural and mechanical properties, which made them attractive for applications in several fields. They have been used since a few decades ago because of its magnetic properties and now the mechanical ones have captured the interest of the scientific community.

The objective of this project is to produce and characterize a Pd-based metallic glass, more specifically $Pd_{77}Si_{16.5}Cu_{6.5}$, using different techniques. An Arc-Melting device, a setup that produces an electric arc employed to melt the constituent elements into balls, and a Melt-Spinner, a rapidly quenching machine to produce micrometer thick ribbons, were utilized for production of ribbons. In order to test the sample quality, they were analyzed with the Scanning Electron Microscopy (SEM) technique, capable of extract the actual composition with a small error.
As characterization techniques, we employed Inelastic Neutron Scattering (INS) to unveil some of their vibrational properties.

Also, a second prefabricated alloy, $Ce_{70}Al_{10}Ni_{10}Cu_{10}$, was characterized using a Dynamic Mechanical Analysis (DMA) which gave us information about its mechanical properties. Two fundamental parameters were found: the glass transition temperature and the fragility of the material.

This project contains two basic parts: production and characterization, where the above mentioned methods and their results are explained. Furthermore, each part contains its own conclusions.

Finally, the project conclusions are presented as a summary of the whole project with the most important data and some suggestions for further research on these exciting materials.

MOTIVATION AND ACKNOWLEDGEMENTS

The main reason why I decided to do this project was the journey to Grenoble that it involved, specifically to the Institut Laue-Langevin (ILL) and European Synchrotron Radiation Facility (ESRF). Not every day one is offered the possibility to go to a Synchrotron and work with professionals of the sector.
Leaving this fact aside, this project offered me many other advantages: it represented my first chance to work with researchers, I would know all about a new kind of materials, the metallic glasses, I would work directly in laboratories using a great variety of machines and see how a researchers life is (which is one of my most seeked interests).

My personal goal was to learn as much as possible about metallic glasses and to prove the abilities acquired during my studies at college.

I am sincerely proud of the result of this project and about what I have learned.

I want to give especial thanks to Jorge Serrano for offering me this project and for convincing me to do it, it was an easy task indeed. I would also like to thank his help throughout the project lifetime.

I want to thank other people who helped me too: Eloi Pineda, Jens Suck, Miguel Ángel González, Daniel Crespo, Trinitat Pradell and Pere Bruna.

Finally, I dedicate this project to my parents, Santiago and Lorenza, who have always helped and supported me since the first day.

INDEX

INDEX OF FIGURES

INDEX OF TABLES

INTRODUCTION

The world we live in has become more and more comfortable thanks to scientific discoveries and subsequent technological developments. Industrial production costs had continually become lower and that affects directly mankind life.

There have been several industrial revolutions caused by material science advances. The first one was the process to mass-produce steel inexpensively, in the 1800s. This led to the production of factories, automobiles, railways and other goods. The second one, in the 1900s, was the extremely low cost of plastic production. The cost of manufacturing was reduced by more than ten times. Silica material produced a revolution in informatics which entailed an increase in mankind comfort.

Now, metallic glasses rise to lead the following revolution: they combine the strength of steels and the elasticity of plastics between other great properties. Their industrial applications lay on sports goods, medicine, mechanical, electronics, jewelry and much more.

The aim of this research work is to learn about metallic glasses and properties by performing experiments using different techniques and then compare our results with previous tests of two specific alloys: $Pd_{77}Si_{16.5}Cu_{6.5}$ and $Ce_{70}Al_{10}Ni_{10}Cu_{10}$. These alloys were investigated using Inelastic X-ray Scattering technique in order to obtain the fragilities. Those fragilities were found to be m = 73 for the first alloy and m = 26 for the second. One objective of this project is to find the fragility for the Ce-based alloy using a dynamical mechanical analysis. Another goal is to find the density of vibrational states in the Pd-based amorphous alloys consisting of bars and ribbons and analyze the differences between both shapes.

This paper is divided in four parts. The first one explains what the metallic glasses are and how their physics work, stepping in their history and so in their mechanical properties and current applications.

The second part describes the whole production process done to get the Palladium-based compound; from the mass calculations until the production of the metallic glasses ribbons by briefly explaining arc-melting and melt-spinner synthesis methods.

The third section delves with the characterization techniques. From each one, there is different information to be found. Scanning Electron Microscopy: the true composition of the Palladium-based compound; Inelastic Neutron Scattering: the density of vibrational states of Palladium-based compound and Dynamic Mechanical Analysis tests: the fragility and mechanical properties of the Cerium-based compound.

Finally, there is a set of conclusions formed with all the concepts, results and analysis performed in this work.

CHAPTER 1. METALLIC GLASSES

1.1 History

The first metallic glass (MG) obtained by rapid quenching techniques was the alloy Au80Si20. It was made by W. Klement (Jr.), Willens and Duwez in 1960 at California Institute of Technology, Caltech [1]. They found that undercooling uniformly and rapidly enough (106 K/s) a molten metal could prevent its atoms from nucleation process and fail to crystallize. At that time, they could only produce metallic glasses with simple and specific forms like ribbons or wires. The maximum thickness reachable was less than one hundred µm.

In 1969, Chen and Turnbull formed amorphous spheres of ternary Pd-Ag-Si, Pd-Cu-Si or Pd-Au-Si at critical cooling rates of 100 K/s to 1000 K/s [2].

Since then on, larger critical thicknesses, i.e. the maximum thickness in which the material is still able to become a glass, have been achieved. Also, the cooling rates have been reduced and multi-component casting with critical cooling rates between 1 K/s to 100 K/s has been realized in Tohoku University and Caltech.

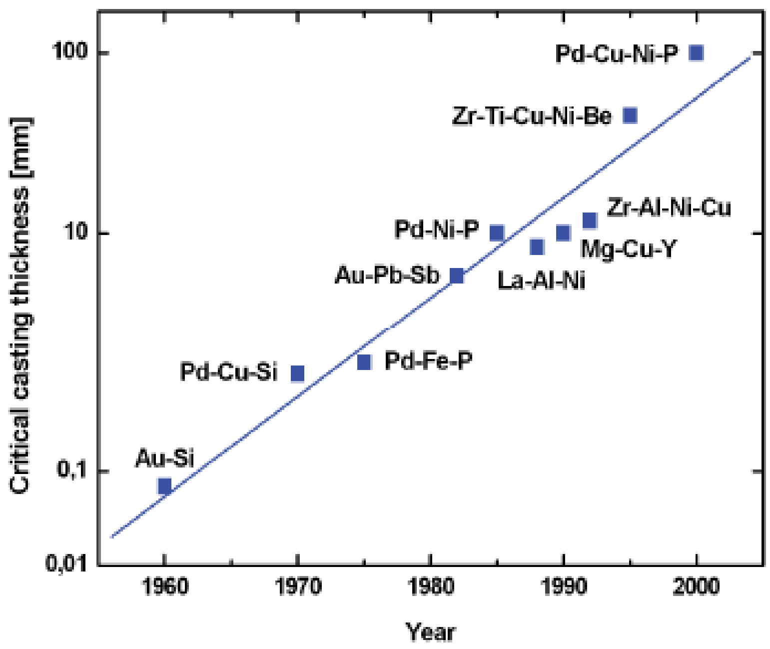

Fig. 1.1 Chronology of alloy discoveries and their critical casting thickness.

Alloys of lanthanum, aluminum and copper were found to be highly glass-forming in 1988.

In the 1990s, however, new alloys were developed that form glasses at cooling rates as low as 1 Kelvin per second. These cooling rates can be achieved by simply casting into metallic molds. These "bulk" amorphous alloys can be cast into rods of up to several centimeters in thickness (the maximum thickness depending on the alloy) while retaining an amorphous structure. The best glass-forming alloys are based on zirconium and palladium, but alloys based on iron, titanium, copper, magnesium, and other metals are also known. Many amorphous alloys are formed by exploiting a phenomenon called the "confusion" effect. Such alloys contain so many different elements (often a dozen or more) that, upon cooling at sufficiently fast rates, the constituent atoms simply cannot coordinate themselves into the equilibrium crystalline state before their movement is stopped. In this way, the random disordered state of the atoms is "locked in".

In 1992, the first commercial amorphous alloy, Vitreloy 1 (41.2% Zr, 13.8% Ti, 12.5% Cu, 10% Ni, and 22.5% Be), was developed at Caltech, as a part of Department of Energy and NASA research of new aerospace materials. More variants followed.

In 2004, two groups succeeded in producing bulk amorphous steel, one at Oak Ridge National Laboratory, the other at University of Virginia. The Oak Ridge group refers to their product as "glassy steel". The product is non-magnetic at room temperature and significantly stronger than conventional steel, though a long research and development process remains to be done before the introduction of the material into public or even military use [2].

1.2 Physical principle

A metallic glass is a metallic alloy with disordered atomic and static structure. It presents a short range order (SRO) and lacks a long range order (LRO). The glass is obtained from a metallic liquid being cooled rapidly by a quenching technique. This prevents the atoms from moving to more stable positions so they cannot order themselves, nucleation does not occur and the solid fails to crystallize. The resultant material has neither crystals nor grains so it is considered homogenous. The viscosity is inversely proportional to the specific volume. It increases as the second is reduced.

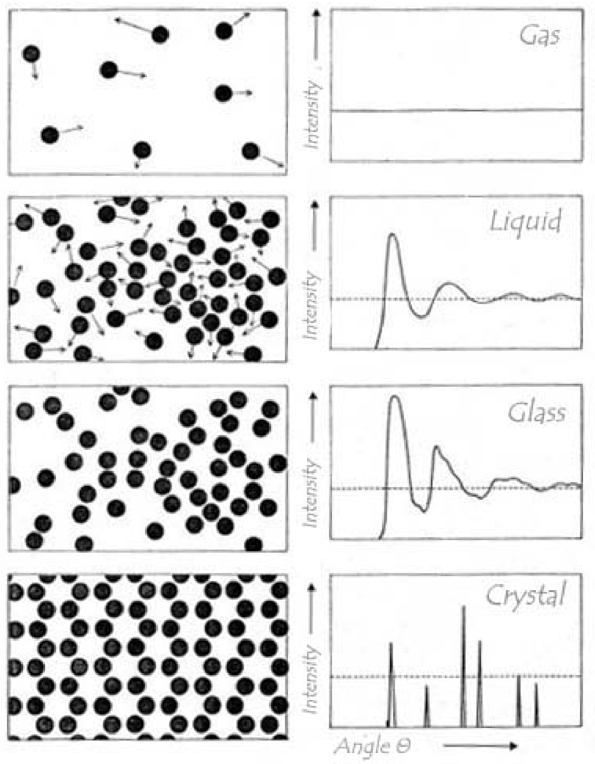

Fig. 1.2 Scheme of different states and their respective pattern using X-ray diffraction.

From figure 1.2 it can be seen that the glassy state resembles liquid phase but the atoms have not speed vector, they are still. The results of an X-ray diffraction study reveal no preference of arrangement in gas state, but maximum in crystalline state. The θ angle at the peaks reveals dominant crystallographic planes. The liquid and the glassy state have similar patterns with no preference or clear peaks in the graphs. However, they present broad bands that show the existence of short-range order.

Besides the difference in structure, glasses exhibit a completely different behavior upon heating.

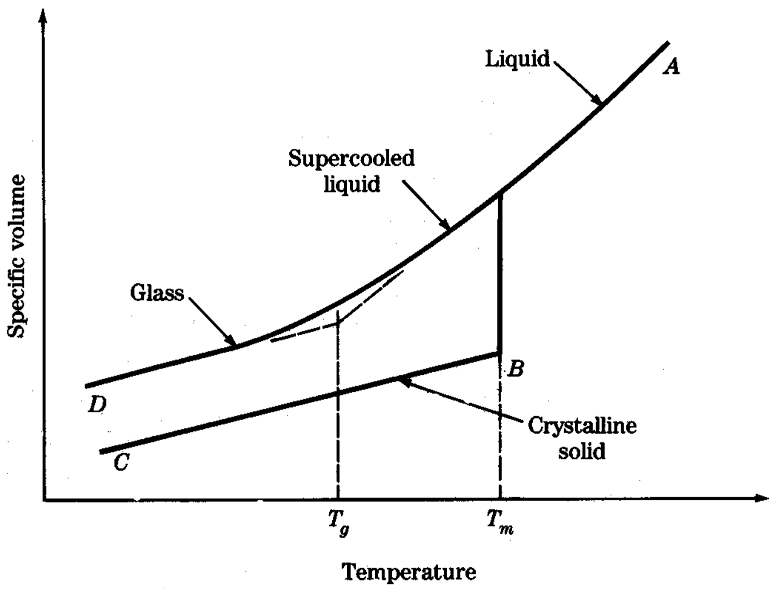

Fig. 1.3 The theoretical Specific volume vs. Temperature graph in glasses.

Figure 1.3 shows the behavior of glassy elements when cooling. At point A the compound is in a liquid phase and the atoms move randomly. As temperature goes down the specific volume of the alloy decreases and the material compacts. When the temperature reaches the melting temperature (Tm) the material has two possible options:

On one hand, if the temperature decreases with slow rate the molten alloy starts to nucleate into little crystals to finish forming a crystalline solid (point B). The specific volume is abruptly reduced maintaining the same temperature due to the phase transformation and the enthalpy of the alloy is also changed. As temperature continues going down the solid keeps compacting itself in a stable phase (point C).

On the other hand, if the rate of decreasing temperature is fast enough, the material enters a metastable phase in which it is still a liquid (supercooled liquid). In this phase, the atoms lack enough time to reorder and the mobility of them is reduced due to the compression of the material. When the temperature goes below the glass transition temperature (T_g) the atoms cannot move freely longer, they can only vibrate, and the result is a glassy stable state (point D). Underneath T_g the nucleation process is not possible.

The parameter that better describes the ability to form glasses is the so called glass forming ability (GFA). One says that a system has a larger GFA when the critical thickness in which a glass can be casted is larger. This, in turn, is related to the stability of the material. The higher the GFA is the larger ability the material will have to vitrify. The thermodynamic variable that measures the stability is the Gibbs free energy (G). It depends on the atomic disorder and the internal energy:

$$G = U + pV - TS = H - TS \qquad \textbf{(1.1)}$$

The states with less G are more stable. It is seen that at constant pressure the materials tend to be at a state of minimum G.

In metallic glasses, the GFA increases when the alloy consists of many components because of the “confusion principle”. When the multinary alloy is melted and rapidly cooled, each component tries to crystallize in its own pattern so it makes every element difficult to crystallize. It is obvious that the more elements are putted the more difficult is for them to achieve any order.

Inoue proposed three empirical rules to determine or improve the GFA of the alloys [3]:

- The alloy has to have three or more elements. Thus, the complexity of the structure is higher and it gets more difficult to obtain any long range order.
- The atomic radius of the principal components has to be quite different (~12%). In this way, high packing density and smaller free volume is achieved.
- The compound may have negative heat of mixing between the principal components increasing the energy barrier at the liquid-solid interface and decreasing atomic diffusivity so that the elements can mix between them; this retards local atomic rearrangement and the crystal nucleation rate, extending the supercooled liquid temperature range and prolonging the time the molten metal stays in the undercooled state.

When a MG is heated their atoms return slowly to the most stable positions. The viscosity descends to a minimum and then rises up again as the material crystallizes.

1.3 Properties

This work is concerned with mechanical properties. Some of them are described below:

Brittleness: ability to break without deformation.

Ductility: ability to be drawn out into wire or threads before rupture. It is also a measure of plasticity.

Elasticity: ability to return to the original shape after the load is removed.

Elastic limit: the point where the material starts to deform plastically. It can also be expressed in terms of yield strength.

Hardness: resistance to plastic deformation.

Plasticity: ability to deform permanently without breaking or rupturing.

Resilience (U_R): ability to absorb energy elastically

Strength: resistance to deformation under load.

Toughness (U_T): amount of energy absorbed until rupture.

Yield strength (σ_y): the stress point when the material starts to deform plastically.

Young's modulus (E): the division between tensile stress and tensile strain. In a stress vs. strain graph, it is the slope in the elastic region. Out of it, it is no longer available.

The ***fragility*** must be defined separately from the mechanical properties since it is the most interesting parameter in this project to be found.
The concept of fragility was defined from the law that describes the change of the viscosity with the temperature approaching the glass transition temperature, T_g. It is highly material-specific and has led to the classification of glass-forming materials. The ***kinetic fragility***, **m**, is directly related to the slowing down of the dynamics and it is defined in terms of shear viscosity η [6].

$$m = \lim_{T \to T_g} \frac{d\log(\eta)}{d(T_g/T)} \qquad \textbf{(1.2)}$$

Thus, **m** is an index of how fast the viscosity increases while approaching the structural arrest at T_g, the temperature at which the structural relaxation time $\tau \sim$ 100 s.

Compared to other materials, metallic glasses show good properties in general. They have high strength, high hardness, high elastic limit, high resilience, high toughness between others.

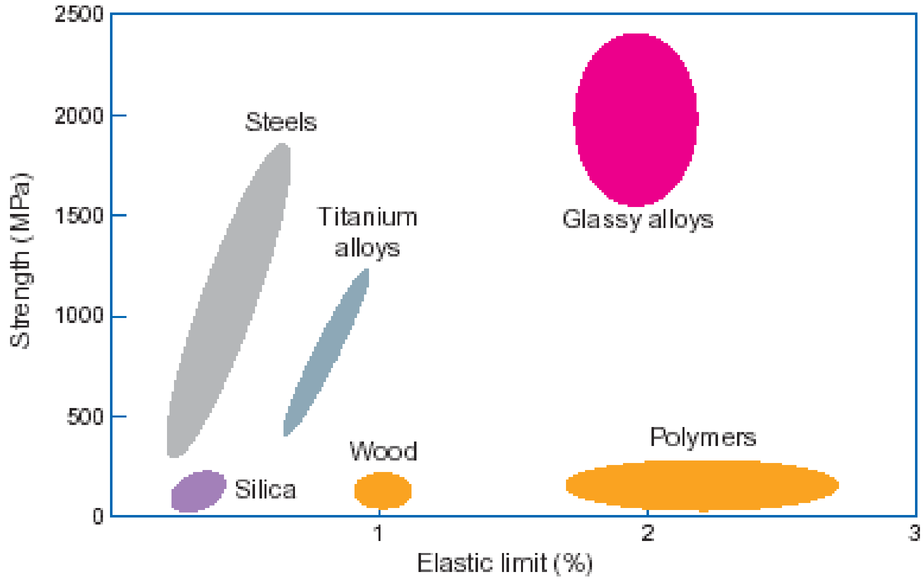

Fig. 1.4 Comparison of glassy alloys with other materials in an elastic limit vs. strength graph.

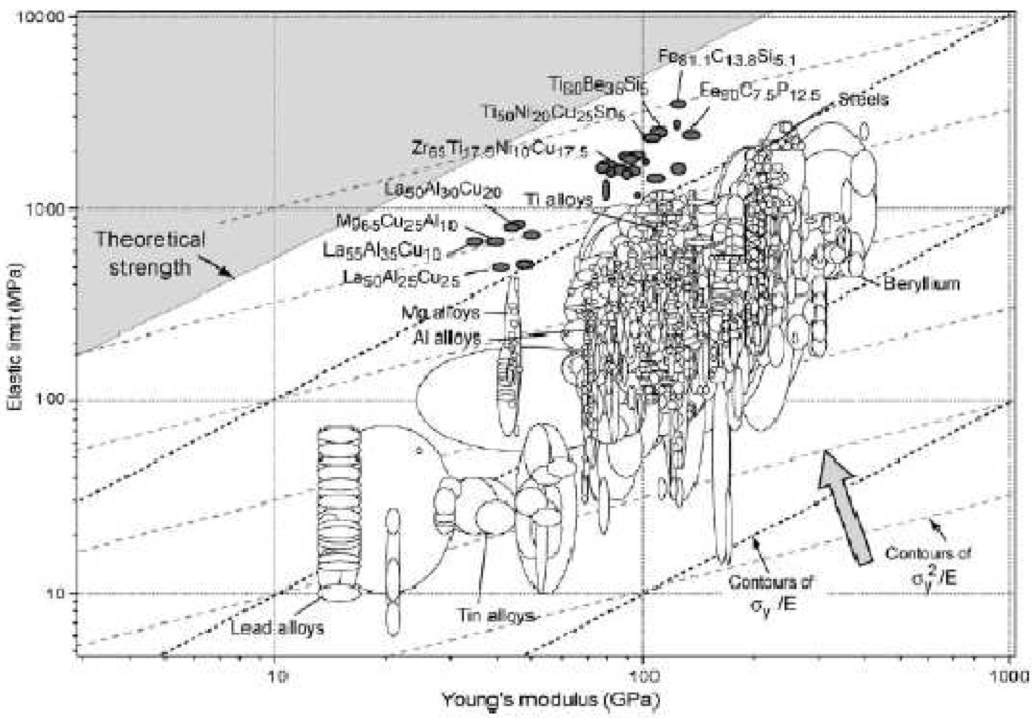

Fig. 1.5 Change in the elastic limit as a function of the Young's modulus.

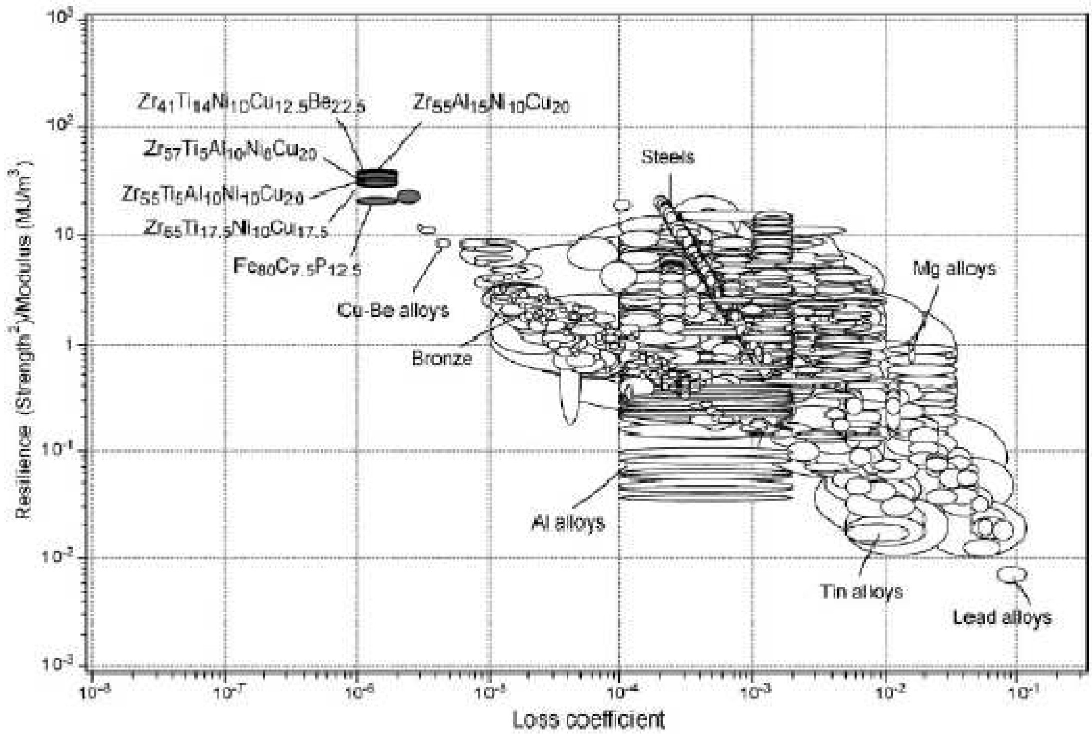

Fig. 1.6 Resilience vs. Loss coefficient.

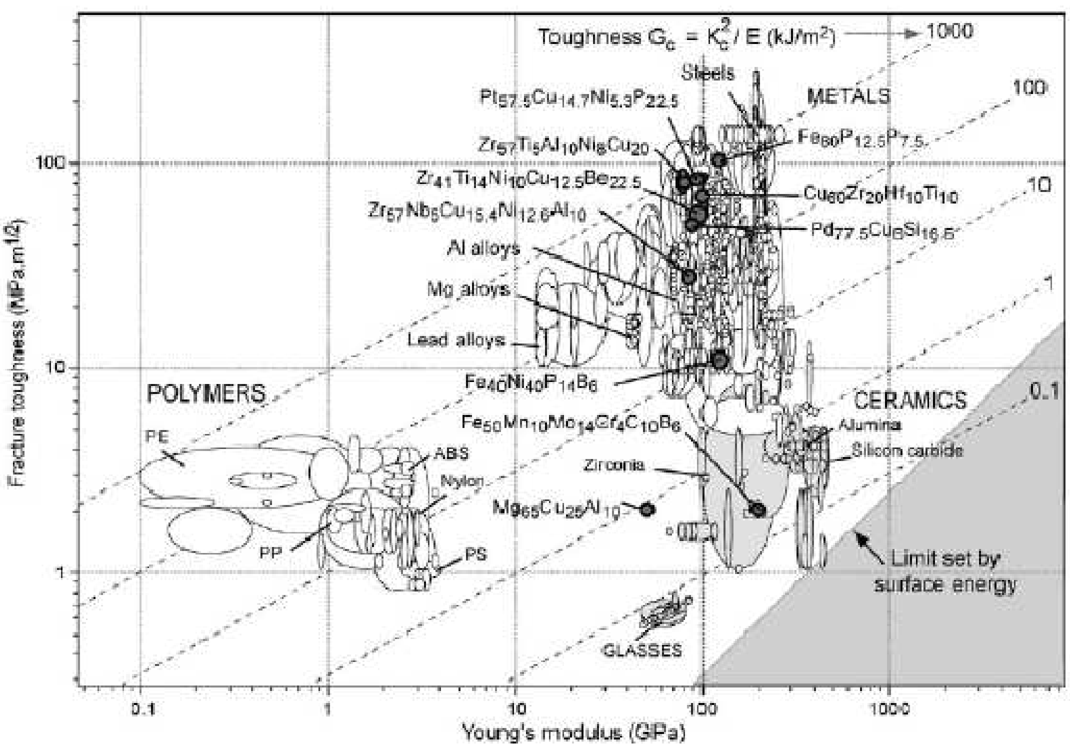

Fig. 1.7 Fracture toughness vs. Young’s modulus.

Most of the mechanic characteristics of these materials come from two aspects: the disorder of the atomic structure and the lack of grains. Since the MGs have a randomly atomic structure, dislocations do not take place. This means that there are neither favorable nor undesired directions to deform, this leading to high yield strength and a homogenous plastic deformation. Nevertheless, metallic glasses present localized shear bands at ambient temperature that causes a strain softening phenomenon and prevents a stable elongation in tension. The lack of grain causes a great-polish ability so all the metallic glasses can have a better finish.

The following is a summary of most of the MG's properties divided in attractive and unattractive according to its attributes:

Table 1.1 Summary of attractive and unattractive properties of MGs [5].

Attributes	Attractive	Unattractive
General	• Absence of microstructural features	• Cost of components and processing • Optimization of GFA prevents other optimizations
Mechanical	• High hardness, yield strength, specific strength and resilience per unit volume and mass • Low mechanical damping • Fracture toughness and toughness can be very high	• Large localization of shear bands (0 ductile in tension) • Fracture toughness and toughness can be very low • Possibly to become more brittle by annealing • Small process-zone size means larger components may fail in brittle manner
Thermal	• T_g < T_c for some MGs, allowing processing as a supercooled liquid	• Instability above T_c limits high temperature use
Electrical and magnetic	• High magnetic permeability • Resistivity is nearly independent of temperature	• Relatively high magnetostriction gives energy loss in oscillating field
Chemical	• Corrosion resistance	
Environmental	• Some compositions biocompatible	• Not easily recycled once in a product
Processing	• High precision and finish in casting	• Slow production rate due to the need for

	• Thermoplastic forming permitted	vacuum die-casting
Aesthetic	• High polish • High durability	
Potential markets	• Aesthetic (high-end life-style products) • Favor µm-to-mm scale structures	• Current high cost of material and processing limits applications to those with high value-added

1.4 Known applications

Although metallic glasses are still far to conquer the industries, humans already give use to them. As a soft magnetic material, metallic glasses are used in transformer cores, magnetic read-heads and magnetic shielding.

Another example is the golf club head. With a high strength-to-weight ratio, different shapes and sizes can be created. The material is so strong and elastic that transmits up to the 99% of the energy to the ball (instead of the 77% from Titanium alloys). Similarly, this application is also employed in tennis where the high stiffness gives 29% more from the total return energy. Other uses of coating may be fishing rods, hunting bows, guns, etc.

Fig. 1.8 Golf club heads can be made with metallic glasses.

Fashion takes profit too from metallic glasses. With the high polish ability and resistance to abrasion and corrosion they fit perfectly as jewelry.

The applications reach medicine field where the ophthalmology scalpels can be casted with MGs. They have greater quality, more durability and are sharper. As new scalpels are made from the same mold (with microscale casting accuracy) its manufacture is more consistent and they are ready for use.

Even so, they are still expensive. Similar applications may be knives and razor blades and prosthesis which need to last [7].

Fig. 1.9 Femur prosthesis made with MGs.

Metallic glasses are applied at defense too. Military materials with specific properties, such as strength, lightness and resistance to tension and high temperatures, can be made. A typical use could be shielding.

In mechanics and electrics field, the MGs may be used in springs and clubs. Its high elastic energy storage per unit volume and mass and the low damping makes them so suitable for springs. The features of lack of grain and high hardness gives them an opportunity to be molded or etched into metallic-glass surface to make masters for reproducing ultra-high-density digital data. Micro electro-mechanical systems (MEMS) could be the perfect field to exploit them. At a small scale like MEMS operate the low ductility is no longer a problem so the main properties rise up to fit perfectly with these systems. Gears are the typical mechanical piece that hangs so much load. With metallic glasses, their teeth won’t break that easy.

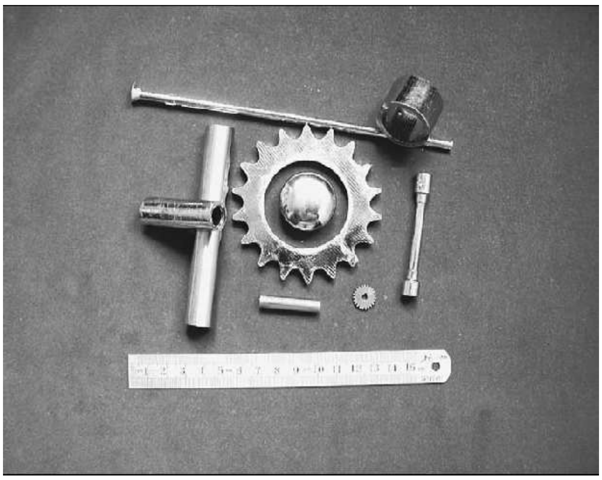

Fig. 1.10 Metallic glasses can be molded into little machinery pieces like screws or gears that may resist high tensions.

Finally, Metallic glasses are of great interest in terms of structural materials due to their mechanical and chemical properties like the high yield strength and the corrosion resistance, respectively, adding the ease of bulk-casting processes achieved. Unfortunately, its high cost and the difficulty to mass-produce in larger scales restricts them to small components. However, a reduction in MG production costs is expected, using cheaper or less pure materials.

CHAPTER 2. SAMPLES PRODUCTION

2.1 Choice of case studies

Many metallic glasses alloys have been produced all over the world and each one had its own interesting peculiarities. This case will center in two alloys already studied by different means. These alloys are $Pd_{77}Si_{16.5}Cu_{6.5}$ and $Ce_{70}Ni_{10}Al_{10}Cu_{10}$.

The first one is an alloy widely studied, specifically the Pd-Si combination. In this case, the objective is to compare the previous results from IXS experiments with INS ones to be obtained in Institute Laue-Langevin in Grenoble. Twenty grams of the requested compound are needed to run the INS tests.

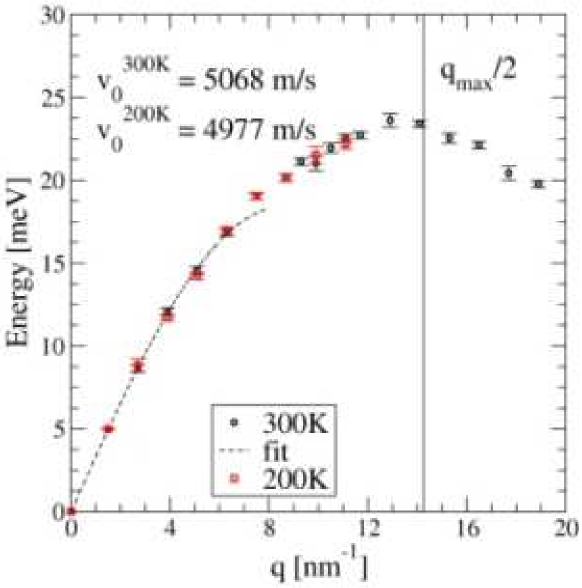

Fig. 2.1 IXS results for $Pd_{77}Si_{16.5}Cu_{6.5}$ alloy.

The second alloy is already created by W. H. Wang and also studied with many techniques. Consequently, there is no need to produce this alloy. This compound may be exposed to Stress-Strain tests and Temperature-Frequency test over the DMA machine. The objective is to find the fragility by measuring the changes in the loss modulus as a function of temperature and frequency and compare with the one obtained from IXS experiments (m = 26).

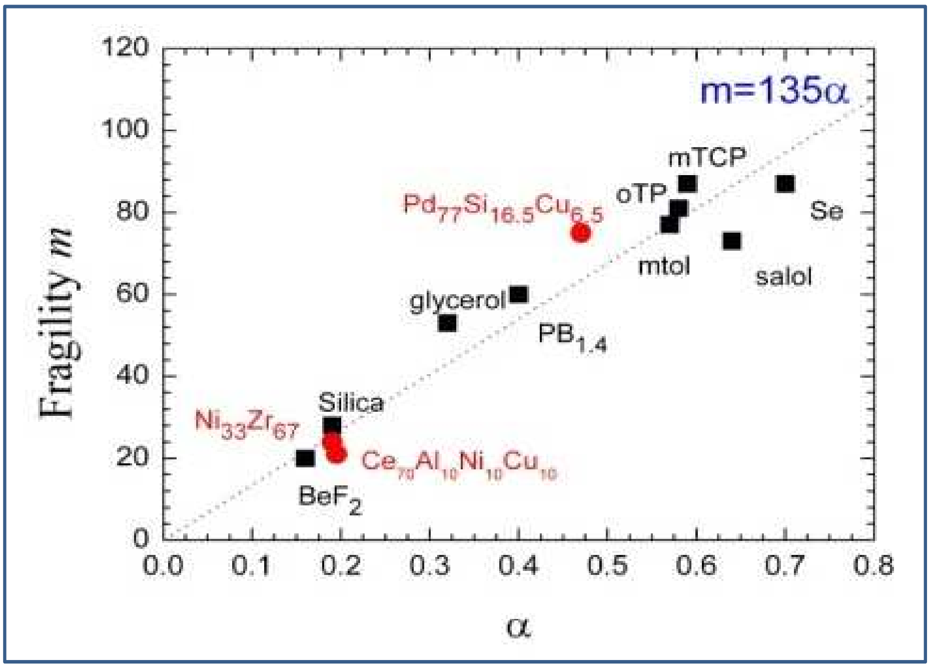

Fig. 2.2 Fragilities chart containing both alloys.

2.2 Preparation of compounds

To create the $Pd_{77}Si_{16.5}Cu_{6.5}$ glassy alloy is recommended to get high purity materials separately in order to reduce the errors in the process. The purities of these materials (Pd, Si and copper) are 99,9%, 99,999% and 99,9% respectively.

The method to obtain the exact mass for each element is as follows. The final mass (2 g), the atomic percentages (Palladium: 77%, Silica: 16.5% and Copper: 6.5%) and the atomic weights (106.42 g/mole, 28.086 g/mole and 63.546 g/mole respectively) are already known. The first thing to do is to calculate the atomic mass of the compound summing the multiplications of atomic masses and atomic percentages of each element.

$$Compound\ Atomic\ Weight = \sum_i^n (m_{Ai} * \%A_i) \qquad \textbf{(2.1)}$$

The atomic weight of the compound results to be 90.70808 g/mole. With this, the total amount of moles is calculated by dividing the atomic weight of the compound by its whole mass, in this case, two grams. The total moles are 0.022.

Then, multipliy again the atomic percentages to the moles to obteain the quantity of atoms for each element (Palladium: 0.017 moles, Silica: 0.0036 moles and Copper: 0.0014 moles). Afterwards, we multiply each quantity by its atomic weight in order to obtain the resultant mass for the three elements.

Finally, the final masses are 1.8067 g for Palladium, 0.1022 g for Silica and 0.0911 g for Copper (these masses sum up 2 grams).

In order to obtain that masses, some workshop time is required. The elements were cut, filed and weighed with the aim to approximate as close as possible to the original masses.

The mean mass for the 15 samples is 1.8066±3.71E-4 g for Palladium, 0.1022±1.65E-4 g for Silica and 0.091±1.1E-4 g for Copper.

Table 2.1 Resultant masses (in grams) of each element and Atomic % variation.

Sample	Palladium	Silica	Copper	Total	New Atomic %
Theoretical	*1.8067*	*0.1022*	*0.0911*	*2.0000*	*77.00 – 16.50 – 6.50*
1	1.8065	0.1025	0.0911	2.0001	76.96 – 16.54 – 6.50
2	1.8070	0.1021	0.0911	2.0002	77.01 – 16.49 – 6.50
3	1.8066	0.1025	0.0910	2.0001	76.96 – 16.55 – 6.49
4	1.8063	0.1024	0.0912	1.9999	76.96 – 16.53 – 6.51
5	1.8068	0.1024	0.0911	2.0003	76.97 – 16.53 – 6.50
6	1.8071	0.1022	0.0910	2.0003	77.00 – 16.50 – 6.49
7	1.8064	0.1023	0.0911	1.9998	76.98 – 16.52 – 6.50
8	1.8065	0.1022	0.0912	1.9999	76.99 – 16.50 – 6.51
9	1.8061	0.1021	0.0912	1.9994	77.00 – 16.49 – 6.51
10	1.8070	0.1023	0.0909	2.0002	77.00 – 16.52 – 6.49
11	1.8072	0.1020	0.0909	2.0001	77.04 – 16.47 – 6.49
12	1.8067	0.1021	0.0910	1.9998	77.01 – 16.49 – 6.50
13	1.8062	0.1021	0.0912	1.9995	77.00 – 16.49 – 6.51
14	1.8061	0.1021	0.0912	1.9994	77.00 – 16.49 – 6.51

2.3 Arc-Melting

An Arc-melter is a machine used to melt the elements and fusion them into the desired compound. This technique uses two electrodes with a potential difference between them to generate an electric arc which enables to obtain temperatures up to 3273.15 K. At these temperatures, most of the components subjected may melt with ease.

A tungsten electrode is used because of its high melting point (3682.15 K). The elements are placed in a base and closed into a pure Argon atmosphere environment.

Actually, there is a three times purgation consisting in -1 bar relative vacuum pressure and then the Argon filling. An ocular protection is mandatory due to the high energy ultraviolet radiation that can damage severely the retinas.

Fig. 2.3 An Arc-melter furnace and control pad.

For the generation of the electric arc a VCC machine is needed in order to apply gradually a 70-90 A current meanwhile the tungsten electrode points a titanium ball to catalyze the reaction. Titanium is a strong absorber of oxygen when heated, and it is also employed as a final indicator of the quality of the Argon atmosphere. Then, with the help of a command rod, the arc can be moved at wish. When the melting is done, the first thing to do is to extract the Argon atmosphere to eliminate possible gasses formed during the melting. Afterwards, the sample is removed and the chamber is cleaned with ethanol, sandpapers, brushes, etc.

The main annoyances found are basically two: some balls may remain so separated that the arc cannot reach to join them and that compound pieces can stick on the tungsten electrode.

The samples were melted at the Arc-melter furnace in pairs with the exception of the last three that were melted together and the first sample that was put alone. Once the material is melted and cooled it has the shape of approximately a sphere. The melted samples were also weighted as it can be seen from table 2.2.

Table 2.2 Weights of the melted samples.

Sample	Original weight [g]	Ball Weight [g]	Efficiency
1	2.0001	1.9306	96.53%
2	2.0002	1.9737	98.68%
3	2.0001	1.9590	97.95%
4	1.9999	1.9638	98.19%
5	2.0003	1.9836	99.17%
6	2.0003	1.9773	98.85%
7	1.9998	1.9610	98.06%
8	1.9999	1.9677	98.39%
9	1.9994	1.9788	98.97%
10	2.0002	1.9799	98.99%
11	2.0001	1.9818	99.09%
12	1.9998	1.9263	96.32%
13	1.9995	1.9591	97.98%
14	1.9994	1.9366	96.86%

As seen in the table 2.2 the general efficiency of this process is really high as the minimum singular efficiency is 96.32%.

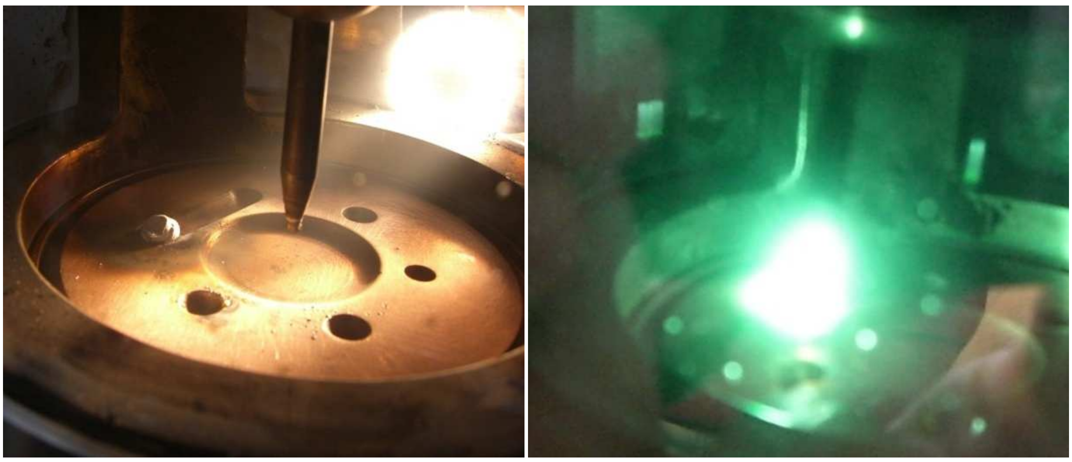

Fig. 2.4 Image of the interior chamber with the internal light and with the arc melting a sample.

2.4 Melt-Spinning

This is one experimental technique for metallic glasses production. A copper coil heats the content of a crucible by induction.

When it is melted there is a decompression of two chambers (the chamber holding the crucible must have lower pressure, both chambers are filled with Argon) and the material is injected to a cooled spinning copper wheel. The alloy is supercooled rapidly and a ribbon is made.

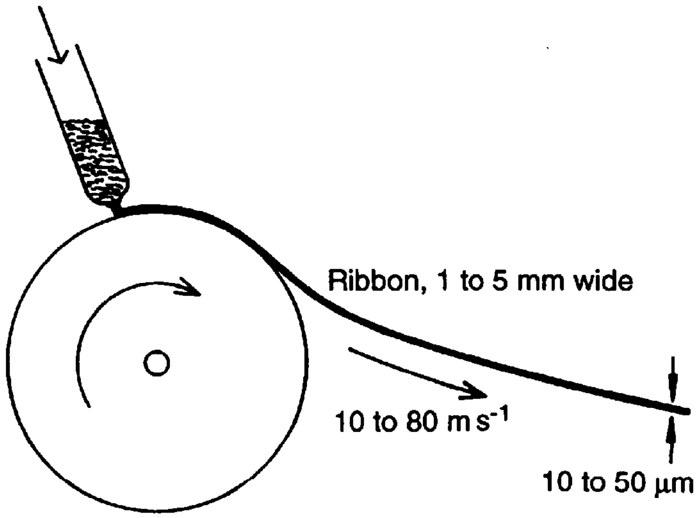

Fig. 2.5 Melt-spinner sketch.

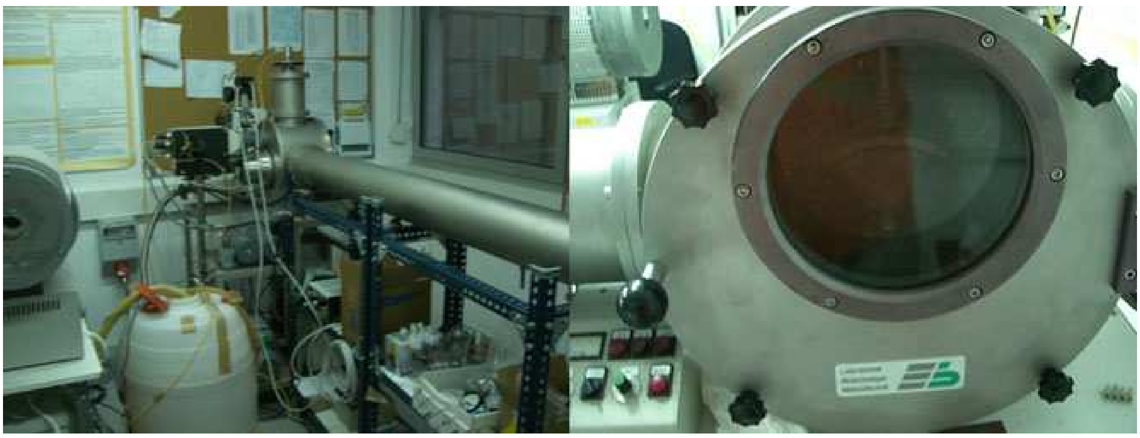

Fig. 2.6 The Melt-spinner at EPSC, Castelldefels.

The temperature of the melted alloy can be displayed thanks to an infrared pyrometer. The emissivity of the material (0.2 for this case) must be introduced and then the whole instrument shall point the main source of heat to determine the temperature with precision. The maximum temperature reached is 1423.15 K with normal values among 1323.15 K.

Fig. 2.7 An infrared pyrometer.

The parameters used to produce these ribbons are the following:

- A bottom crucible hole diameter of 1 mm.
- A distance between the wheel and the crucible of 1.05 or 1.15 mm.
- A chamber pressure of 400 mbar.
- An injection pressure of 800 – 900 mbar.

With these parameters the ribbons may have a width between 1 and 2 mm and a thickness between 25 and 50 µm.

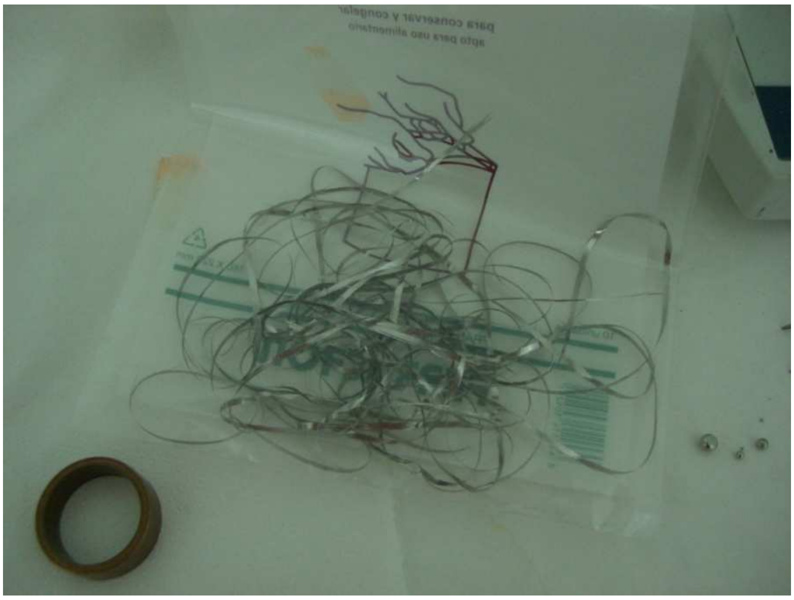

Fig. 2.8 The output ribbon has a shiny silver color.

Compared with the Arc-melting, this technique is much less efficient. The maximum efficiency founded is 67.06%. The remainder material has spread into many useless forms like mini balls and hair-like particles.

Table 2.3 Weights of the melted samples and resulting ribbons.

Sample	Ball weight [g]	Ribbon weight [g]	Efficiency
1	1.9306	1.0600	54.91%
2	1.9737	2.3600	60.01%
3	1.9590		
4	1.9638	2.1808	55.25%
5	1.9836		
6	1.9773	2.6066	66.19%
7	1.9610		
8	1.9677	2.6465	67.06%
9	1.9788		
10	1.9799	2.4361	61.49%
11	1.9818		
12	1.9263	3.2539	55.89%
13	1.9591		
14	1.9366		

CHAPTER 3. CHARACTERIZATION AND ANALYSIS

3.1 Previous results

There are many ways to characterize each of the materials properties. The composition, the atomic structure state (whether is crystalline or amorphous), its Young's modulus and other properties will be studied and analyzed in this section.

The Pd-based alloy was studied using a Scanning Electron Microscope test to find out the actual composition of each sample of the series, which should not be far from the nominal composition: $Pd_{77}Si_{16.5}Cu_{6.5}$.

The second, Ce-based, alloy was studied in a Dynamic Mechanical Analyzer machine to obtain its mechanical properties. This compound was analyzed already by many scientists. Below, there are some properties found in by W.H. Wang by differential scanning calorimetry techniques (DSC) [10]:

- T_g: 359 K
- Critical diameter: 3mm
- Young's modulus = 30.3 GPa
- Shear modulus = 11.5 GPa
- Poisson's ratio = 0.313

3.2 Scanning Electron Microscopy (SEM)

3.2.1 Description

This technique uses a high-energy electron beam to generate detailed two-dimensional images of the sample topography or surface, as well as to find out the chemical composition.

Fig. 3.1 A scanning electron microscope commonly known as the electric microscope.

The beam begins at the electron gun where a Tungsten cathode is excited by an anode below to thermo-ionically emit a ray of electrons. Tungsten is commonly used because of its high melting point and low vapor pressure but another possibility is Lanthanum Hexaboride. The electron beam, with a typical energy from a few hundred eV to 40 keV, is focused by one or more magnetic lens to a very small resolution, 1 to 5 nm, granting a magnification of the sample up to x250,000 (6 orders of magnitude).

Electrons are focused with magnetic lens. The ray can get wider or narrower within the ranges. Furthermore, it can move along the x-y plane thanks to the scanning coils which can deflect the ray in those directions. When the electron beam impacts the sample, the electrons lose energy by repeated random scattering. The energy exchange between the electron beam and the sample results in reflection of high-energy electrons by elastic scattering, emission of secondary electrons by inelastic scattering and the emission of electromagnetic radiation in x-ray frequency, each of which can be detected by specialized detectors.

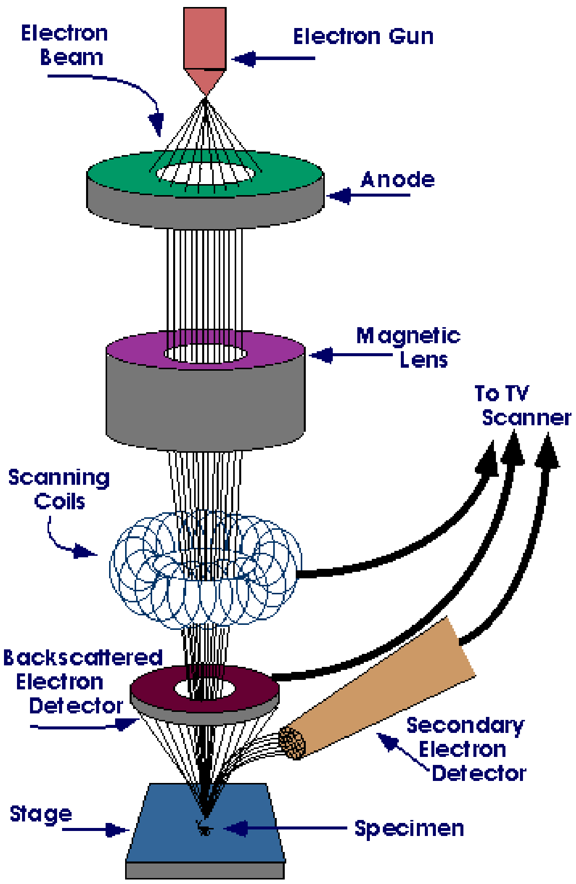

Fig. 3.2 Scheme of the electron beam path and detectors.

3.2.2 The signals

Primary backscattered electrons (BSE): they are the electrons elastically scattered out of the sample domains. The interaction energy is minimal so they have a high kinetic energy and a change in their momentum (the direction of the velocity is changed). The dispersion of these electrons is high enough to reduce the resolution. The quantity of them is lower compared to secondary electrons. However, they can be used to determine the composition of the sample as the BSE increases with the atomic number Z.

Secondary electrons (SE): come from the inelastic scattering of the electron beam. The energy transmission is high and the resulting energy of the electrons is between 0 and 50 eV. Every single SE can generate many more because it causes more collisions in its trajectory. The formation of a topographical image is due to local variations of the electron emissivity at the surface so they are used to generate a surface image of the sample.

X-rays: they can be detected with a special method called Energy Dispersive X-ray Spectroscopy (EDX or EDS). This method is used to find the chemical composition.

It analyzes the x-rays emitted by a material excited with electrons in a physical phenomenon called x-ray emission. The electrons from the beam impact into other orbital electrons throwing them away.
Then, other electrons from higher orbitals fall to these and a photon is emitted with an energy given by the following equation:

$$\Delta E = \hbar \upsilon \quad \textbf{(3.1)}$$

Where v is the frequency of the photon and ħ is Planck's constant. The amount of x-rays is counted and arranged in different energies into a spectrum. Each material has its own electron binding energies so there are no two elements with any electron binding energy equal. They could be similar but not the same.

The larger the amount of photons received for an element, the larger the atomic percentage of that element. Finally, the real composition is found with an error depending on the machine and external factors. This uncertainty typically amounts to 1-2 AT%.

3.2.3 Sample Preparation

Depending on the conductive or insulator properties of the samples, they are prepared in a different way. If they are not metallic, they are coated with gold powder so that they become conductive.

Afterwards, the samples are arranged in a sticky layer and then glued on a button. There is a round base that can stand six buttons. One of them is brass with a cobalt circle at the middle used to calibrate the stability of the beam, which depends mainly on the state of the tungsten wire. The supports are earthed to avoid electric charge of samples. The base is placed in the sample chamber at a vacuum pressure of the order of 10e-10 bar.

Fig. 3.3 A round base and four buttons with ribbon fragments.

3.2.4 Experimental procedure

It took place at “Serveis Cientifico-tècnics de la Universitat de Barcelona” in Barcelona with the machine JEOL JSM-840 (with a maximum error in composition of ±2%). The samples were placed as explained before.

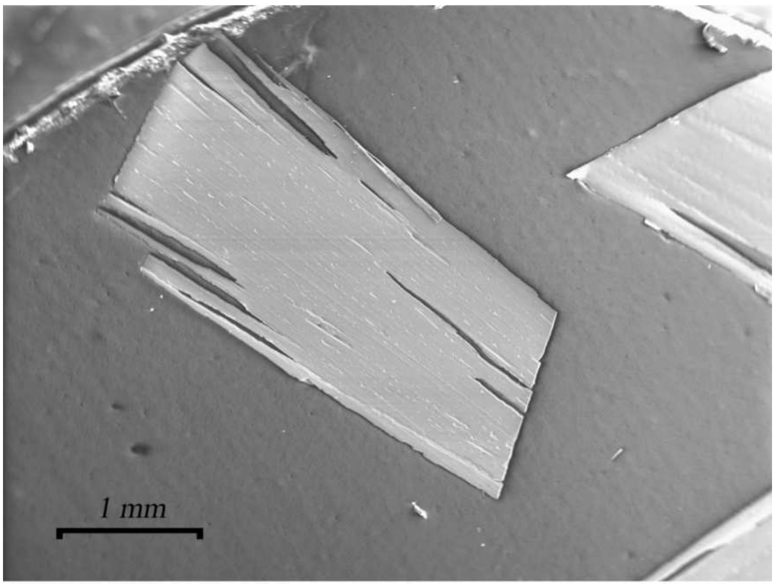

Fig. 3.4 Image taken of a ribbon piece.

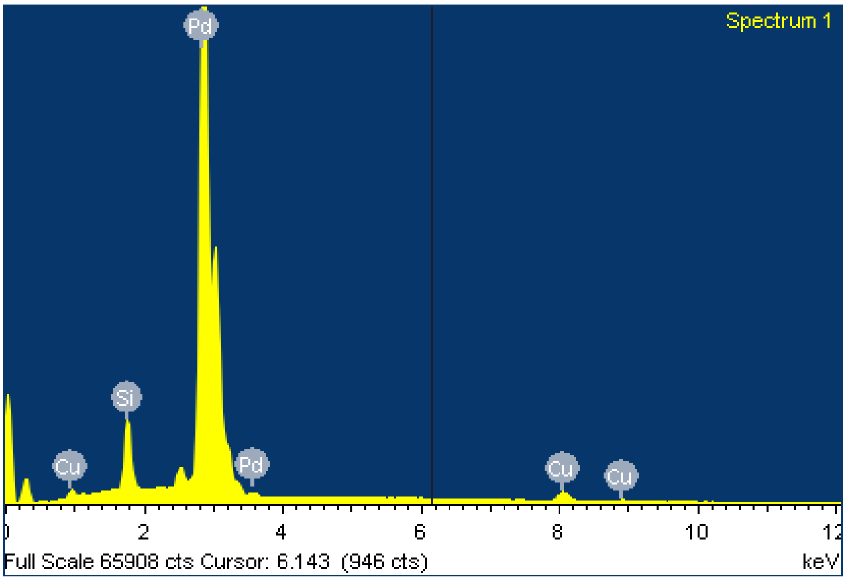

Fig. 3.5 An energy dispersion spectrum of a sample.

The figure 3.5 is a typical spectrum for element analysis obtained using Energy Dispersion Spectroscopy technique (EDS). The abscissa axis is the electron binding energies in keV. Each element has some representative levels in this spectrum. The ordinate axis represents the intensity; the larger it is, the larger quantity of this element is present. The percentage is the average all the intensities.

The table 3.1 shows the characteristic electron binding energies corresponding to the constituent elements of the sample. This table can be used to ascertain the presence of the respective elements in the spectrum of figure 3.5.

Table 3.1 Electron binding energies in eV.

Label	Orbital	Pd	Si	Cu
K	1s	24350	1839	8979
L_{I}	2s	3604	150	1097
L_{II}	2p1/2	3330	99.8	952.3
L_{III}	2p3/2	3173	99.2	932.7
M I	3s	671.6		122.5
M_{II}	3p1/2	559.9		77.3
M_{III}	3p3/2	532.3		75.1
M_{IV}	3d3/2	340.5		
M_{V}	3d5/2	335.2		
N_{I}	4s	87.1		
N_{II}	4p1/2	55.7		
N_{III}	4p3/2	50.9		

Table 3.2 SEM compositional results of all analyzed pieces. The buttons were analyzed during two different sessions, using a different tungsten wiring.

a) Button 1

Session	Sample	Face	Nº	%Pd	%Si	%Cu
1st	1	Shiny	1	79.98	15.27	4.75
1st	1	Shiny	2	80.32	14.54	5.15
1st	1	Dull	1	79.47	15.50	5.02
1st	1	Dull	2	80.22	14.92	4.87
1st	2	Shiny	1	80.15	14.97	4.88
1st	2	Shiny	2	80.26	14.78	4.96
1st	2	Shiny	3	80.41	14.77	4.82
1st	2	Dull	1	80.37	14.67	4.95
1st	2	Dull	2	79.62	15.37	5.01
1st	2	Dull	3	79.91	15.20	4.89

b) Button 2

Session	Sample	Face	Nº	%Pd	%Si	%Cu
1st	1	Shiny	1	80.06	14.50	5.44
1st	1	Shiny	2	79.50	14.97	5.53
2nd	1	Dull	1	79.73	14.72	5.55
2nd	1	Dull	1	79.27	14.98	5.75
2nd	1	Dull	2	78.88	15.64	5.48
2nd	2	Shiny	1	79.39	15.50	5.11
2nd	2	Shiny	2	79.46	15.27	5.26
2nd	2	Shiny	1	79.69	15.07	5.24
2nd	2	Dull	1	79.76	14.73	5.51
2nd	2	Dull	2	79.30	15.03	5.68
2nd	3	Shiny	1	80.75	15.25	4.00
2nd	3	Shiny	2	80.47	15.46	4.08
2nd	3	Dull	1	80.45	15.41	4.15
2nd	3	Dull	2	80.81	14.79	4.39
2nd	4	Shiny	1	80.57	15.31	4.11
2nd	4	Shiny	2	80.87	14.82	4.31
2nd	4	Dull	1	80.53	15.34	4.13
2nd	4	Dull	2	80.66	15.14	4.21

c) Button 3

.

Session	Sample	Face	Nº	%Pd	%Si	%Cu
2nd	1	Shiny	1	79.17	14.53	6.30
2nd	1	Shiny	2	79.98	13.40	6.62
2nd	1	Dull	1	79.10	14.58	6.32
2nd	1	Dull	2	79.01	14.65	6.34
2nd	2	Shiny	1	79.13	14.74	6.13
2nd	2	Shiny	2	79.38	14.54	6.08
2nd	2	Dull	1	79.18	14.32	6.50
2nd	2	Dull	2	79.35	14.28	6.37
2nd	3	Shiny	1	78.85	15.47	5.68
2nd	3	Shiny	2	79.60	14.29	6.11
2nd	3	Dull	1	78.93	14.99	6.08
2nd	3	Dull	2	79.01	15.28	5.71
2nd	4	Shiny	1	79.07	15.17	5.76
2nd	4	Shiny	2	79.13	15.32	5.54
2nd	4	Dull	1	79.07	15.00	5.94
2nd	4	Dull	2	79.11	15.07	5.82

d) Button 4

Session	Sample	Face	Nº	%Pd	%Si	%Cu
2nd	1	Shiny	1	78.47	15.16	6.36
2nd	1	Shiny	2	78.53	15.17	6.31
2nd	1	Dull	1	78.60	15.13	6.28
2nd	1	Dull	2	78.57	15.09	6.35
2nd	2	Shiny	1	78.58	15.28	6.14
2nd	2	Shiny	2	78.59	15.10	6.30
2nd	2	Dull	1	78.59	15.07	6.33
2nd	2	Dull	2	78.44	15.13	6.44
2nd	3	Shiny	1	80.22	14.67	5.11
2nd	3	Shiny	2	80.36	14.52	5.12
2nd	3	Dull	1	80.37	14.36	5.27
2nd	3	Dull	2	80.52	14.39	5.10
2nd	4	Shiny	1	80.24	14.50	5.26
2nd	4	Shiny	2	80.44	14.46	5.10
2nd	4	Dull	1	79.94	14.72	5.34
2nd	4	Dull	2	80.14	14.56	5.30

Table 3.3 Atomic percentages means depending on different parameters.

Type	%Pd	%Si	%Cu
Session 1	80.02	14.96	5.02
Session 2	79.55	14.90	5.55
Button 1	80.07	15.00	4.93
Button 2	80.01	15.11	4.88
Button 3	79.19	14.73	6.08
Button 4	79.41	14.83	5.76
Shiny face	79.56	14.94	5.50
Dull face	79.72	14.89	5.39

Notice that each ribbon presents a dull and a shiny faces, resulting from the contact and lack of contact to the copper wheel of the melt spinner during the production stage.

There is no difference between buttons 1 and 2 and between buttons 3 and 4 but there is between the two sets. That may be due to the way of preparing the samples: cutting the pieces from the same ribbon and sticking them all together in one button until the ribbon is off; that also justifies the fact that the percentages between pieces in the same button are similar.

The atomic concentrations measured during the second day seem to be closer to the nominal. This might be because in the first day of operation the Tungsten wiring was almost worn-out and finally got broken. As the wiring consumes itself the stability of the electron beam becomes poorer and the error increases.

The conclusion drawn from the faces is that the thickness of the ribbons (25 to 50 µm) is so small that the ribbon is homogeneous and concentration variations are too small to be detected with this technique.

3.3 Inelastic Neutron Scattering (INS)

Time-of-flight spectroscopy (TOF) is a technique used to explore vibrational and magnetic properties of materials from the behavior of scattered neutrons in an inelastic process (INS), i.e. with change in energy and direction of propagation [13].

In the case of metallic glasses, INS allows one to determine relevant properties such as the density of vibrational states (VDOS) and the excess of vibrational states that affects the low temperature behavior of specific heat, known as the Boson peak [14].

IN4C is an instrument at Institute Laue-Langevin (Grenoble) which implements this technique. The operation of IN4C is as follows. The source of the neutron beam is the centre of the reactor placed next to the instrument. The neutrons fly in all directions and those that go in the instrument direction must pass through the choppers which let go only the neutrons with a certain speed. The selected neutrons bounce in the monochromator because of Bragg's Law so only those with a desired wavelength are selected and reflected with the right angle. Then, there is a second chopper (so-called Fermi chopper) that must filter again the neutrons by speed. From this setup, one can obtain the energy difference between incident and scattered neutrons, which corresponds to the energy of the atomic vibrations under consideration.
The beam impacts in the sample and most of the neutrons scatter throughout a row of detectors arranged in a 120º arch. The detectors count the number of neutrons and its time of arrival.

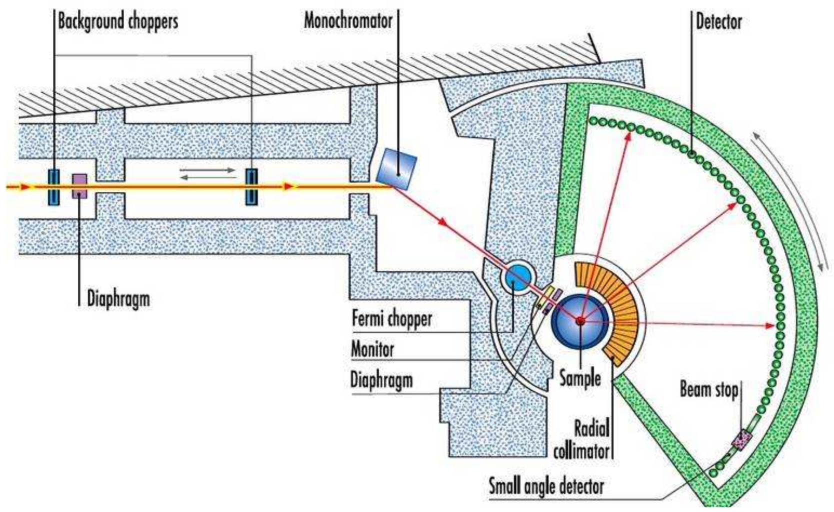

Fig. 3.6 IN4C instrument scheme of operating.

3.3.1 Experimental procedure

In order to calibrate the instrument background a test was run with a Vanadium sample. The samples to study were 14.51 grams of Pd-based ribbons and 10.90 grams of bars with the same composition produced by Jorge Serrano, Eloi Pineda, and Pere Bruna.

The tests are divided into two configurations. The first one corresponds to a neutron incident wavelength λ = 1.26 Ǻ. In this way, the electrons had 51 meV energy. The sample was kept cooled by liquid Nitrogen to a temperature of 210 K. These parameters were used in order to investigate the positive zone in the energy exchange between neutrons and the sample (positive means that neutrons give energy to the sample, creating atomic vibrational modes). The more energy the neutrons have the higher probability is for them to give energy. On the other side, the second experiment was performed with λ = 2.52 Ǻ, i.e. incident neutron energy of 13 meV. The sample was kept at a temperature of 330 K. Thus, the sample is more excited and has many chances to transfer energy to the low energized neutrons.

The resulting data was analyzed by Jens Suck and is displayed below.

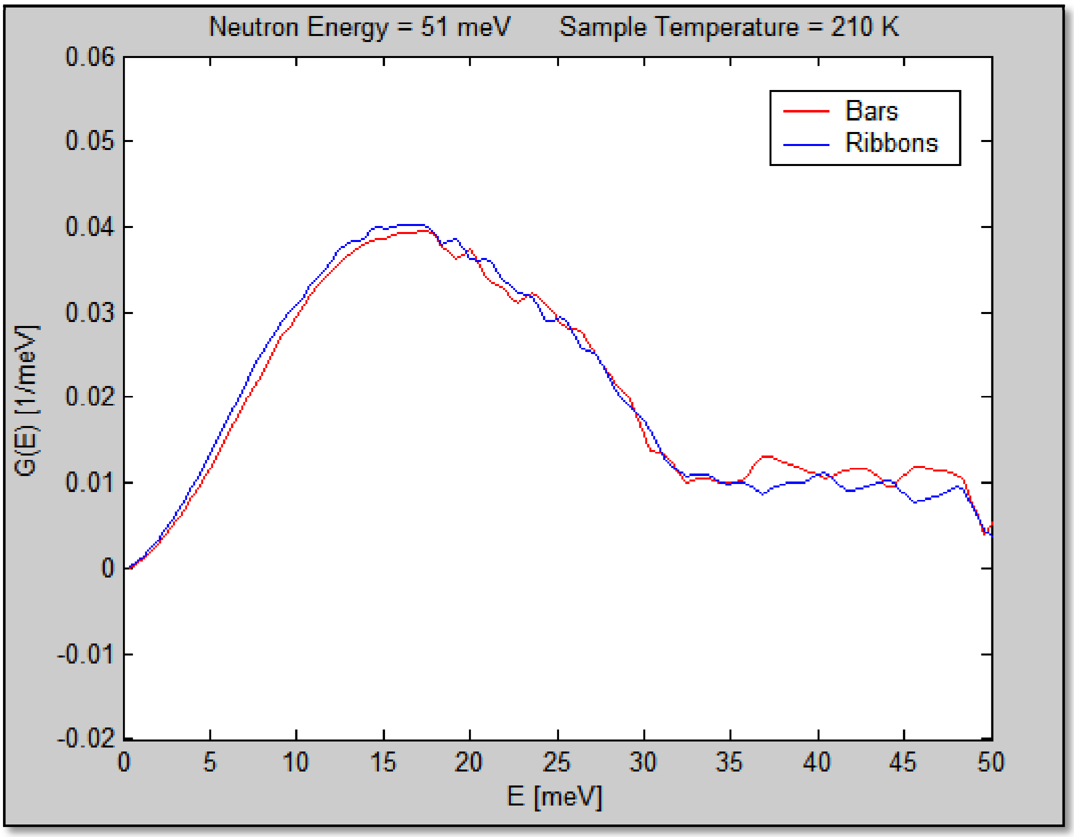

Fig. 3.7 Enlargement of VDOS first test.

From figure 3.7 it can be seen that the density of vibrational states G(E) for bars is slightly lower than that for ribbons until E = 17 meV. Beyond this point, the density of states for bars starts to become larger.

There is a peak of vibrational states at 16 meV with a value of 0.04 meV^{-1}. This value of energy gives information of the fundamental frequency of vibration of the material. This is always the same for all the temperatures but, as temperature changes, the amount of vibrational states at this frequency changes.

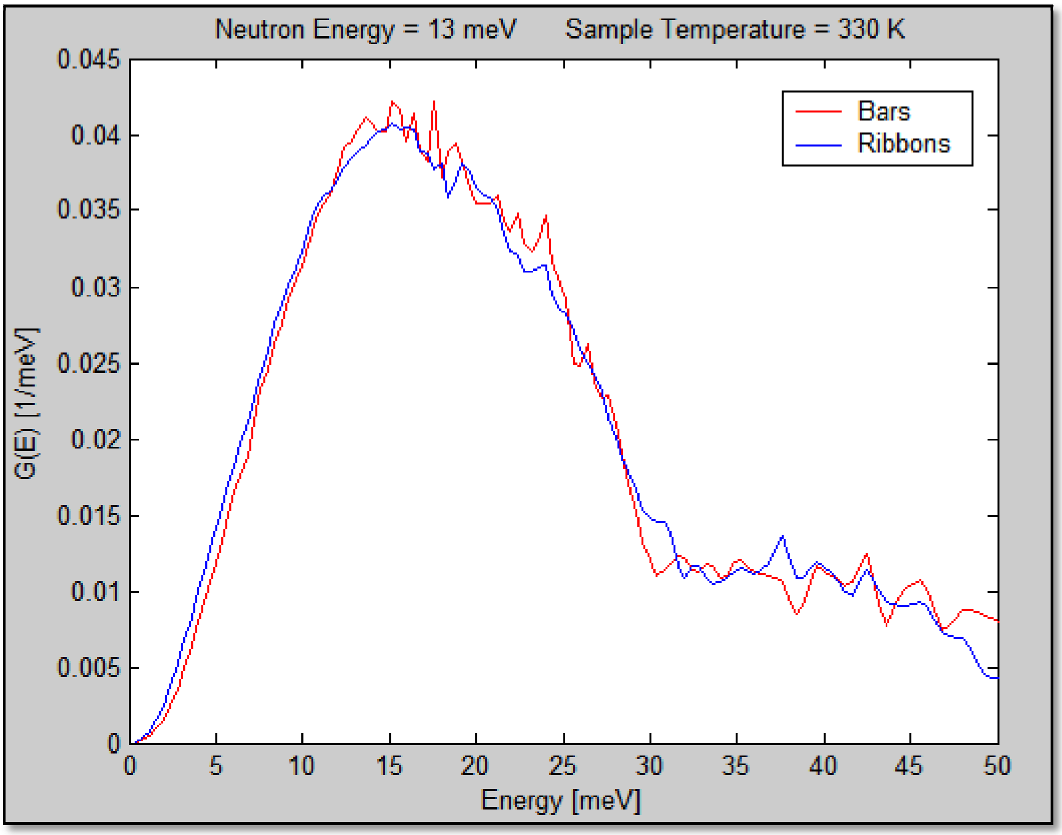

Fig. 3.8 Enlargement of VDOS second test.

The second test is similar to the first but it seems to have better resolution at lower energies. The values of G(E) are higher for bars in the peak, which is placed at the same energy as in the first test: 16 meV. The peak has the same value because both tests have been normalized to 0.04 meV^{-1} but for higher temperatures the peak should be higher since the density of states is proportional to temperature, due to the Bose-Einstein factor.

Comparing both experiments one can see that lower neutron energies have more resolution at low ranges of energy of vibration.

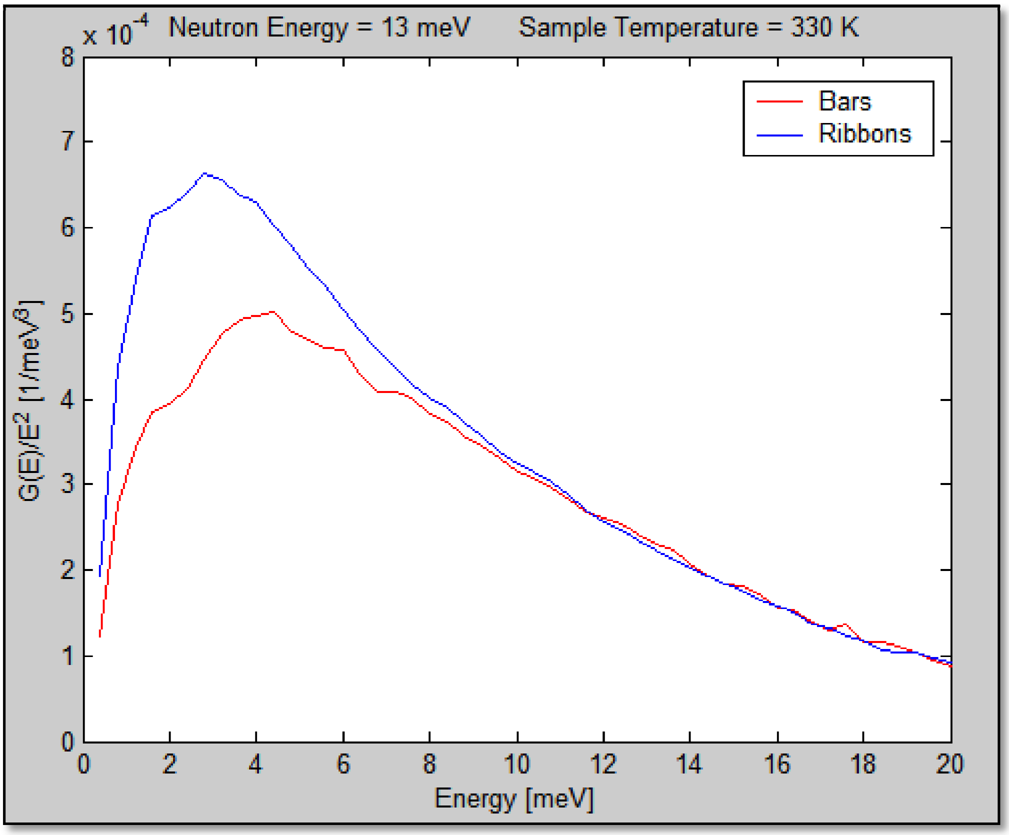

Fig. 3.9 Boson peak for bars and ribbons in second test.

The Boson Peak (BP) is an excess of vibrational states and only occur in glasses. The origin of this peak is still unclear and the only knowledge is that this peak is related to similar peaks observed in the curves of specific heat and conductivity at low temperatures.

Only a BP has been found. It is placed at 3.76 meV in the second test and only corresponds to the bars..

3.4 Dynamic Mechanical Analysis (DMA)

3.4.1 Description

The TA Instruments Q800 Dynamic Mechanical Analyzer (DMA) is a thermal analytical instrument used to test the mechanical properties of many different materials. To make measurements, the test specimen is mounted on one of several clamps, all of which have been designed using Finite Element Analysis to minimize mass and compliance. Basically, a deformation is imposed on the specimen in order to evaluate intrinsic as well as extrinsic mechanical properties of the material (e.g. modulus, damping, creep, stress relaxation, glass transitions, and softening points).

It determines changes in sample properties resulting from changes in five experimental variables: temperature, time, frequency, force, and strain. It operates over a temperature range of -145℃ to 600° C, using heating rates up to 20℃/min and forces from 0.0001 to 18 N. It can be used with samples in bulk solid, film, fiber, gel, or viscous liquid form. Depending on the clamp put the force type changes from tension, compression, shear stress and other. The ribbons analyzed with this machine were all tested with tension clamps.

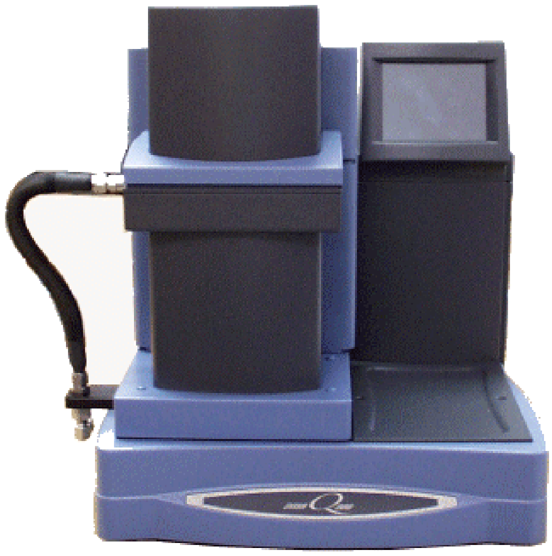

Fig. 3.10 Dynamic Mechanical Analyzer.

3.4.2 Strain-Stress tests

The Strain-Stress curve is a representation of both parameters. It gives much information about the mechanical properties of the sample. In figure 3.11, there is a curve of a sample studied at 300 K (ambient temperature). The force rate must be low enough to let the machine recollect more precise data. All the force rates for these tests were set to 1 N/min. The preload force (the force applied for ribbon initial tension) was 0.005 N.

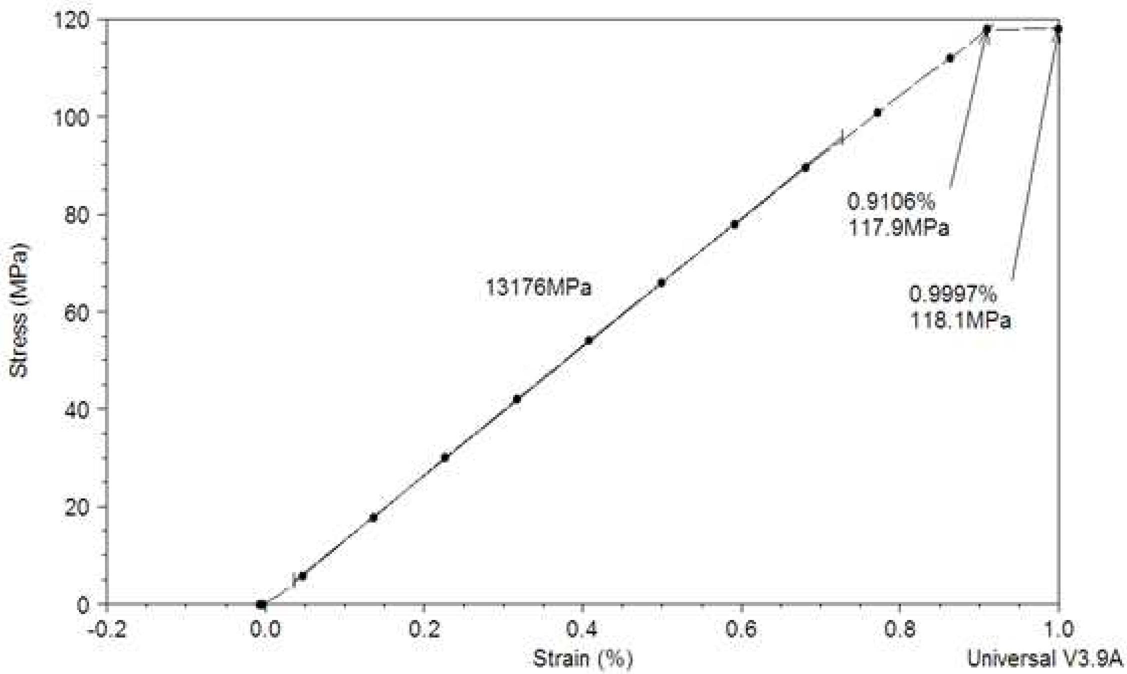

Fig. 3.11 Strain vs. stress graph at 300 K.

This sample has a Young's modulus of 13176 MPa. The elastic region ends at a strain of 0.9106 % with a yield strength of 117.9 MPa. Out of this region the ribbon deforms plastically. This compound is hardly ductile because of the short plastic region.

The total amount of elastic energy that can storage and return (resilience) is (117.9 MPa)2 / 2*(13176 MPa) = 0.527 MJ/mm3 (see equation 3.2).

$$U_R = \int_0^{\varepsilon_y} \sigma(\varepsilon) d\varepsilon = \frac{1}{2}\sigma_y \varepsilon_y = \frac{1}{2}\sigma_y \left(\frac{\sigma_y}{E}\right) = \frac{{\sigma_y}^2}{2E} \quad \textbf{(3.2)}$$

The total energy absorbed before rupture (toughness) is approximately 0.643 MJ/mm^3 (see equation 3.3). The rupture point is placed at 0.9997 % of elongation that makes the sample very brittle.

$$U_T = \int \sigma(\varepsilon) d\varepsilon \quad \textbf{(3.3)}$$

The following experiment consists in Strain-Stress tests of the same composition at different temperatures. It is interesting to observe what happens to the mechanical properties as a function of temperature.

The higher temperature employed in these experiments is 350 K because the T_g found by Wang was 359 K. Thus, above this value the compound test would behave like a composite.

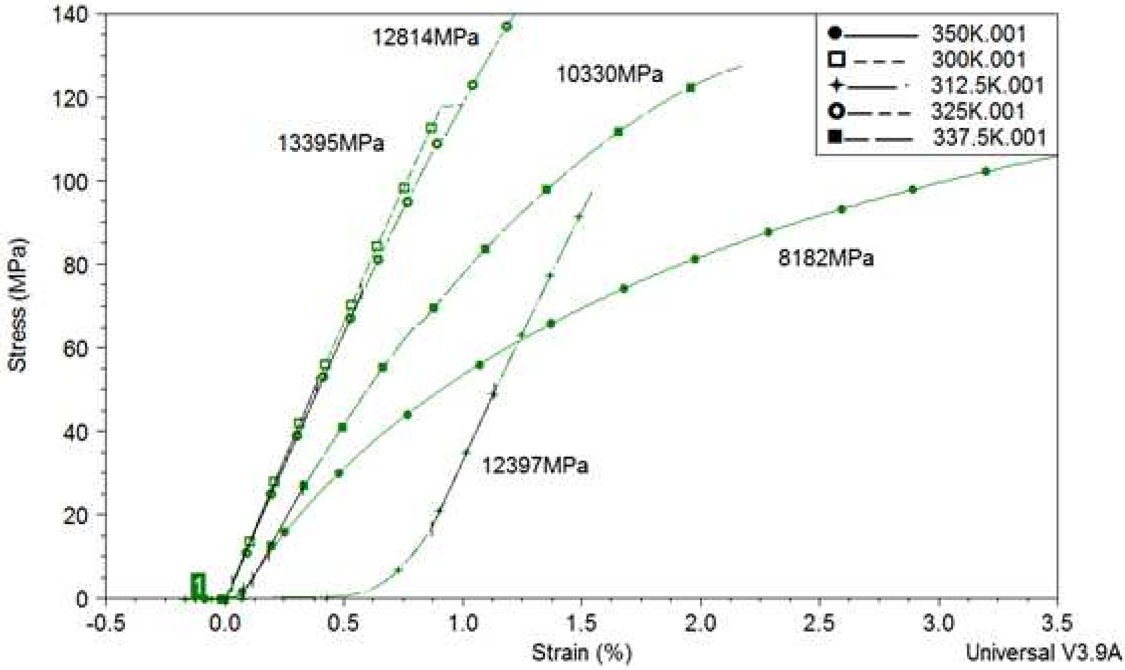

Fig. 3.12 Strain vs. stress curves and their respective Young's modulus at different temperatures.

The figure 3.12 shows five Strain-Stress curves at different temperature. When the ribbons are heated they behave differently. At greater temperatures the Young's modulus becomes smaller so the material becomes more ductile and deforms much more plastically. Larger ductility entails more toughness.

These ribbons were not elastic enough to see whether there was strain softening. In fact, they are quite brittle at low temperatures since they have no yield point.

Table 3.4 Young's modulus of Stress-Strain test at different temperatures.

Temperature [K]	Young's modulus [MPa]
300	13395
312.5	12397
325	12814
337.5	10330
350	8182

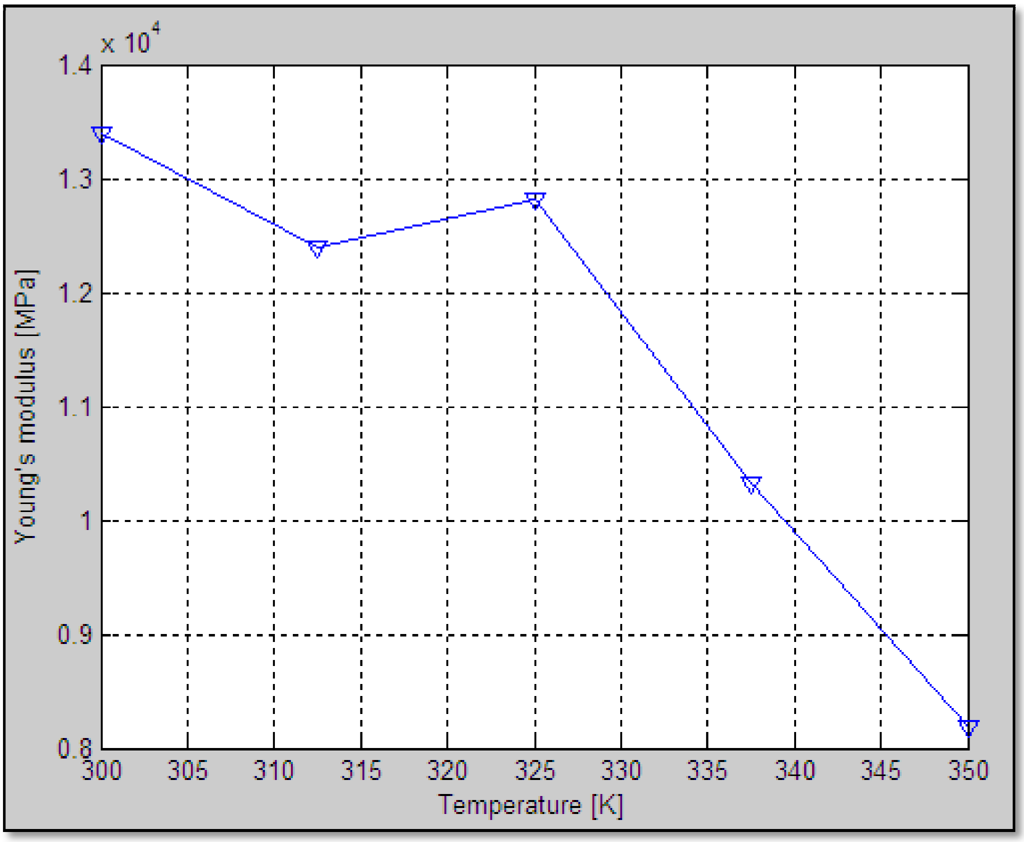

Fig. 3.13 Relation between Young's modulus and Temperature.

The figure 3.13 shows that E is inversely proportional to the temperature. If the 325 K result is not taken into account, the relation seems to be quite linear with a slope of approximately -104 MPa/K. In order to define a stable law, more tests are required. Nevertheless, it's widely known that in normal materials this occurs too. If a common metal is heated, its ductility will grow.

3.4.3 Temperature Ramp tests

During dynamic testing, an oscillatory (sinusoidal) strain (or stress) can be applied to the material and the resulting stress (or strain) developed in the material is measured. If the material is 100 % elastic, the stress and strain signals will have the same phase as the response of the sample is instantaneous (see figure 3.14). On the other hand, if the material shows a 100% viscous behavior, the signals will have a 90º deviation in phase.

Most real-world materials exhibit mechanical responses that are a mixture of viscous and elastic behavior. Thus, they are viscoelastic. For a viscoelastic material, the phase angle will lie somewhere between 0° and 90°.

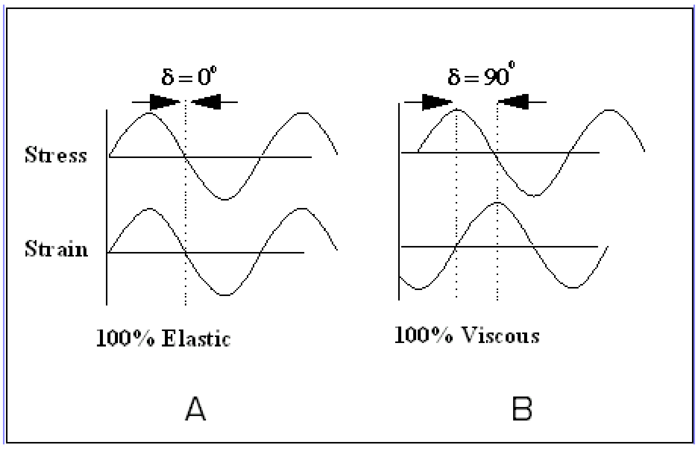

Fig. 3.14 Behavior of elastic and viscous materials.

Furthermore, the temperature grows at a specified rate. This rate must be slow enough so that the temperature dependence can be observed properly. In this case, the chosen rate was 1K/min. This rate had been determined in previous tests performed on similar compositions.

The amplitude of elongation, a controllable parameter, was set to 1 µm so that the deformation was always this value and the stress was calculated each time. It is interesting to know where the elongation is located in the strain-stress curve in order to see whether the ramp starts in the elastic regime.

The intention of this test is to find the glass transition temperatures for different frequencies of oscillation. This will allow one to find out the fragility of the material. In order to find the T_g, the Loss modulus (a measure of viscous response) is needed to be found first.

As the *modulus* is defined as the ratio of stress to strain (stress/strain), the resultant stress generated in a viscoelastic material—also referred to as the *complex stress* (σ* or τ*)—can be used to calculate the *complex modulus* E* or G*. The complex modulus is a measure of materials resistance to deformation. It encompasses both elastic and viscous responses. The power of dynamic testing is that, by using the measured phase angle, the stress can be deconvolved into two parts: an elastic stress (σ’ or τ’), that is in phase with the strain, and a viscous stress (σ” or τ”), that is 90° out of phase with respect to the strain.

The elastic modulus, or *storage modulus* (E’ or G’) and the viscous modulus, or *loss modulus* (E” or G”), can then be calculated directly from the elastic and viscous stress respectively (see figure 3.15).

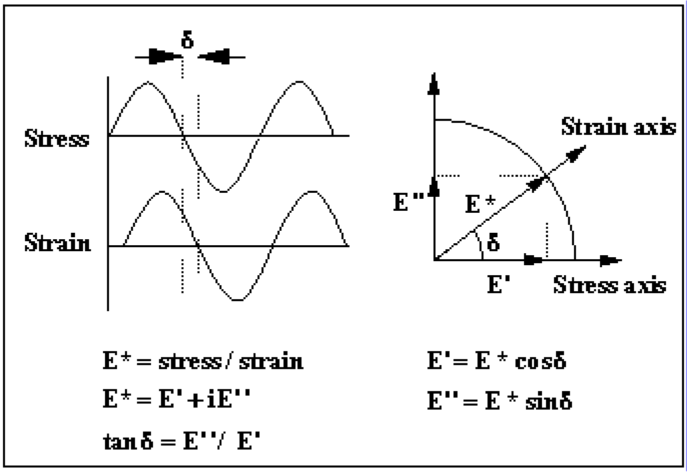

Fig. 3.15 Behavior of viscoelastic materials.

The ribbon chosen to be analyzed is the one with the shortest length. This makes the deformations larger so the probability to be out of the elastic regime increases. The shortest ribbon employed had a length of 13.2255 mm and was tested with a frequency of 32 Hz.

The parameters used for all the Temperature Ramp tests were the following:

- Soak time: 1 min.
- Temperature rate: 1 K/min.
- Maximum Temperature: 398.15 K.
- Preforce: 0.15 N.
- Amplitude: 1 µm.

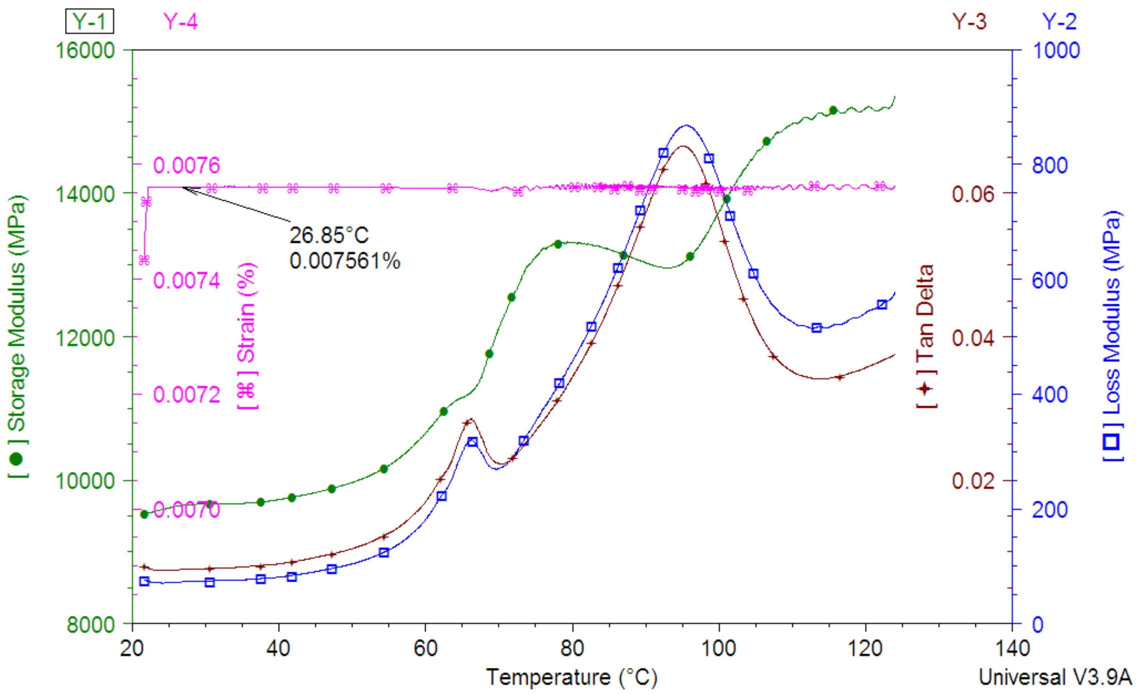

Fig. 3.16 Temperature ramp graph of the 32 Hz sample displaying Storage Modulus, Loss Modulus, Tan Delta and Strain.

For this sample, the resulting strain at 300 K (26.85 ºC) was 0.007561 % so this deformation is elastic (the elastic zone was between 0 and 0.9106 %) and consequently, the previous tests are in a proper threshold of testing.

Theoretically, the T_g for that composition is placed at the maximum point of the Loss modulus curve when the frequency oscillation is 0.01 Hz. To perform this experiment is complicated due to the very low frequency. In order to circumvent this issue, a solution may be getting this value form the extrapolation from a collection of curves obtained for higher frequencies.

The T_g found for 32 Hz lays around 368.15 K (95 ºC). At this point the atoms gain energy progressively and start moving slowly. That movement allows them to organize in more stable positions so the material crystallizes. This process makes the material more viscous until it solidifies completely. Then, the material behaves elastically again, just as a normal crystalline alloy. Furthermore, if the temperature keeps growing up the compound starts to melt so the viscosity increases.

Notice the strain curve. When it reaches the T_g zone it is more difficult to maintain the amplitude to exactly 1 µm due to the changes in the material atomic structure so the strain oscillates more.
The curves of loss modulus at different frequencies and their maximums are displayed in the following figure.

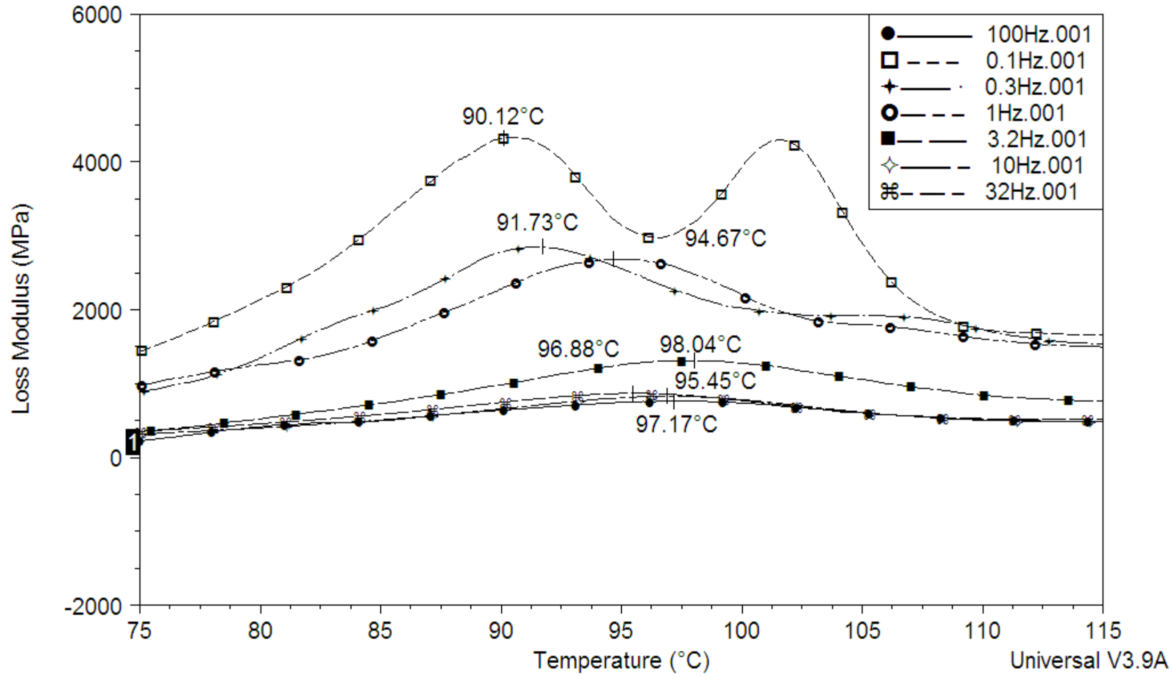

Fig. 3.17 Loss Modulus vs. Temperature graph for different frequencies.

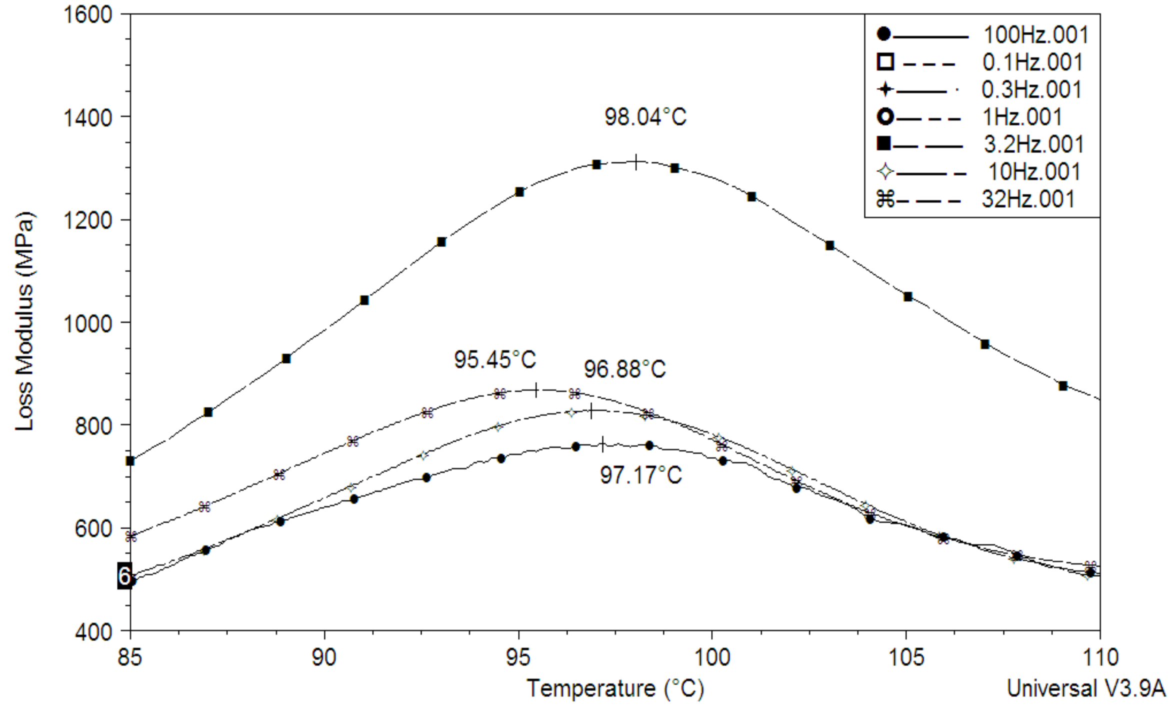

Fig. 3.18 Enlargement of the previous graph.

Table 3.5 Temperatures of glass transition from each frequency test.

Frequencies [Hz]	T_g [K]
0.1	363.27
0.3	364.88
1	367.82
3.2	371.19
10	370.03
32	368.60
100	370.32

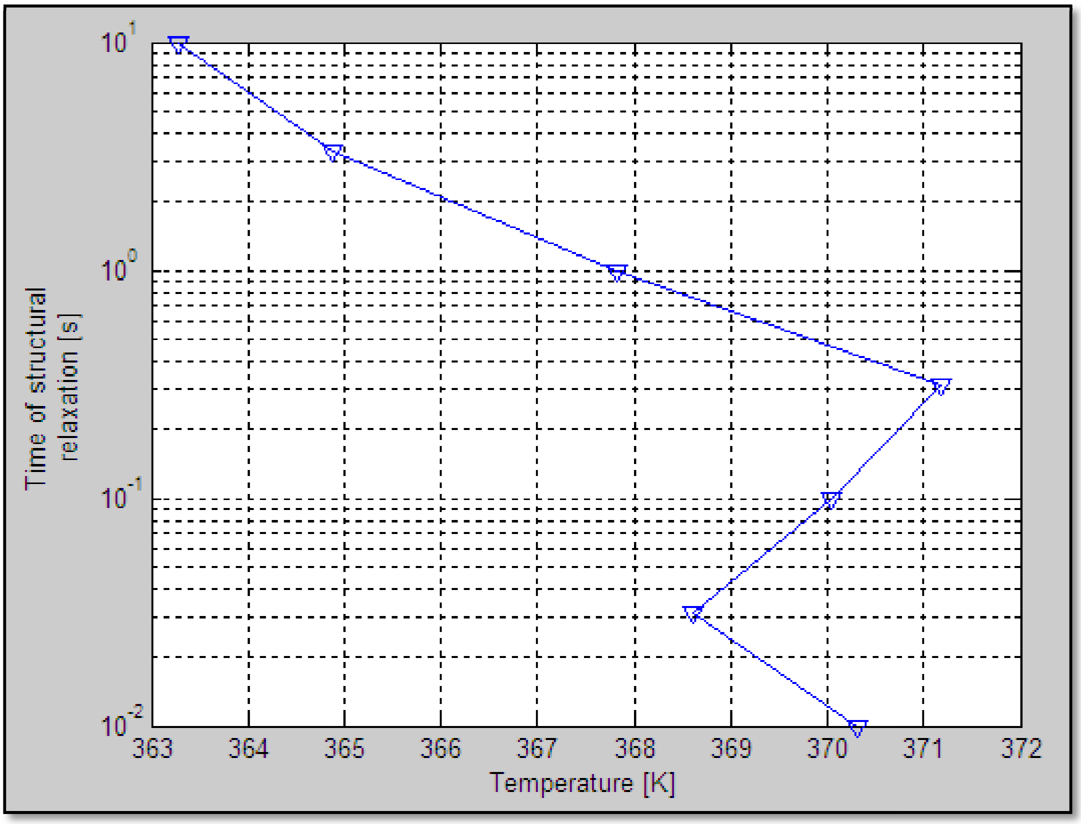

Fig. 3.19 Time of structural relaxation vs. Temperature graph.

It can be seen from the table 3.5 and graph that T_g generally moves upwards as the frequency increases. That curve is not perfectly known so an adjust is required to find the real T_g and fragility for the material. Theoretically, that T_g is defined when the relaxation time is set to 100 s so the result will be extrapolated from the adjust curve since the maximum frequency studied was 10 s.

The function used to adjust the results is the Vogel-Fulcher-Tamman function that describes relaxation time dependency for liquids [16]:

$$\tau(T) = \tau_O \, exp\,(\frac{D\,To}{T-To}) \quad \textbf{(3.4)}$$

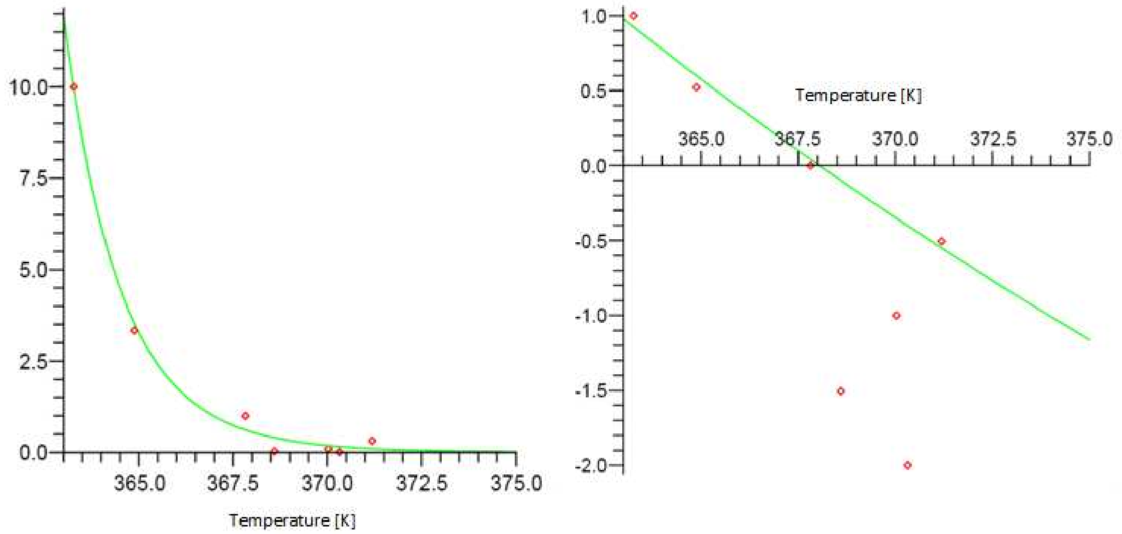

Fig. 3.20 Linear and natural logarithmic VFT function adjustment curves.

The analysis of the fit has been performed by Eloi Pineda at Dept. Física i Enginyeria Nuclear, ESAB, Castelldefels.

The nominal values T_g and m from calorimetry are 359 K and 26 respectively and the resulting values we obtained from dynamic mechanical analysis are 358 K and 84. The coincidence in T_g and the discrepancy in fragility comes from the fact that they are two independent parameters of the linear fit. The slope has resulted to be quite wrong.

Fig. 3.21 Degradation of ribbons.

This may be caused by the oxidation of the ribbons (see in figure 3.21 the degradation occurred in the ribbons, the color has changed from silver to golden and to blue) and by difficulties in the identification of the T_g at each frequency since the crystallization and vitrification temperatures are so close that could have been mistaken. Many other parameters may have compromised the experiments like a bad calibration of the DMA, the bad finish of the ribbons, etc.

Further experiments are underway to corroborate these results.

CHAPTER 4. CONCLUSIONS

The main goal of this project was to learn as much as possible about Metallic Glasses, a new kind of materials. These resulted to be metallic alloys with disordered atomic structure and with interesting mechanical properties unknown for other materials like high Young's modulus and brittleness, high hardness and strength, etc. They also have other attractive properties like corrosion resistance and high durability. Such properties come from the lack of grains and the disorder in the structure.
The second objective was to produce and characterize two alloys by different means.

To create the first alloy, $Pd_{77}Si_{16.5}Cu_{6.5}$, the Arc-Melting technique was used to melt the weighed elements into balls using an electric arc and then, in order to produce ribbons of this compound, put them into a rapid quenching machine called Melt-Spinner. The latter resulted to have less efficiency than the Arc-Melter (67.06% versus 96.32%). The characterization was performed by two means:
The first one is the so called Scanning Electron Microscopy which was used to verify the atomic composition of the ribbons. The so obtained atomic percentages were correct and an extra conclusion was taken in this experiment which is that the stability of the electron ray becomes poorer as the wiring wears.

14.51 grams of ribbon were used with Neutron Inelastic Spectroscopy technique. The objective was to find information about the vibrational properties of the samples. The experiment consisted of two tests, each one with a different neutron energy and sample temperature. The first one, E = 51 meV and T = 210 K and the second, E = 13 meV and T = 330 K resulted to have the maximum of the density of vibrational states occurring at the same exchange energy, of 16 meV. This gives information about the fundamental frequency of atomic vibrations in the metallic glasses under investigation, which is independent from the sample temperature and the incident neutron energy. Furthermore, 10.90 grams of purchased 1 mm diameter bars of the same composition were also analyzed by INS. Similar results were obtained with the difference that the bars had more density of vibrational states at low energies and less at high energies and that there was a Boson Peak in 3.76 meV.
This technique has better resolution at low energies for lower neutron energies.

The second alloy, $Ce_{70}Al_{10}Ni_{10}Cu_{10}$, was melted into ribbons that were subsequently investigated using the Dynamic Mechanical Analysis with two methods.

Firstly, a piece of ribbon was studied with Stress-Strain method. A gradually tension force (5 N/min) was applied at a temperature of 300 K. The results were: a Young's modulus of 13176 MPa, an elastic limit of 0.9106 %, a yield strength of 117.9 MPa, a resilience of 0.527 MJ/mm^3, a toughness of 0.643 MJ/mm^3 and a rupture point at 0.9997 %. This material resulted to be quite brittle.

Afterwards, a similar experiment was conducted at different temperatures (312.5 K, 325 K, 337.5 K and 350 K), all below the glass transition temperature, T_g. A quasi-linear dependence was found between the temperature and the Young's modulus with a slope of -104 MPa/K.

The second method consisted of a study in which an oscillating tensile deformation is applied to the ribbon while the temperature increases at a specific rate (in this case 1 K/min). The strain calculated at 300 K was 0.007561 % so the deformation is elastic. Upon increase in temperature, an increase in the loss modulus is observed up to a maximum, with a subsequent decrease beyond this temperature. The following step is to calculate the temperature corresponding to the maximum Loss modulus for 7 different frequencies of oscillation (0.1 Hz, 0.3 Hz, 1 Hz, 3.2 Hz, 10 Hz, 32 Hz and 100 Hz). The temperatures found were: 363.27 K, 364.88 K, 367.82 K, 371.19 K, 370.03 K, 368.60 K and 370.32 K, respectively. A Vogel-Fulcher-Tamman adjustment function was needed to find the fragility and the true T_g for the material. These were 84 and 358 K respectively. The fragility was far distant from the nominal value (26). That may be due to oxidation of ribbons, a bad calibration, the bad finish of the ribbons, or mixing of the T_g signal with another peak in the loss function due to the crystallization process.

Bearing these results in mind, one can consider the application of this material in concrete sectors such as a sports goods, jewelry, medicine, science and military. These fields take the best properties of metallic glasses for their own interests, e.g. the durability makes the medical prosthesis last longer, the ability to have better finish makes the golden rings more expensive, the high elastic limit permits rackets return more energy, etc.
In fact, these are the current applications because metallic glasses have great properties but their production is expensive and these sectors have enough wealthy to afford it.

In the aeronautical world, metallic glasses could be used in those places where the fatigue plays an important role. Little screws and gears, wing joints or even the new emergent Micro-electro mechanical systems fit perfectly with the mechanical properties of MGs.

Further projects are required to advance this research. The process to find the T_g for each frequency is still uncertain and could be studied better as well as methods for increasing the efficiency of the Melt-Spinner.
The Inelastic Neutron Scattering is a difficult matter which needs entire projects only for this science.

In terms of environmental impact, the execution of this work has entailed the production of low quantities of metallic glasses and the use of other already produced (less than 1kg in total).
These materials have been tested in three different experiments: SEM, INS, DMA. The most dangerous test is INS since the ribbons and the bars are put in a neutron flow that can turn the sample radioactive. The radiation levels read after the experiment were found to be lower than the minimum to consider them radioactive waste.

Finally, the resultant materials can be thrown in a normal metal recycling container. The gases used throughout the techniques were Argon and Nitrogen which are inert so there is no need to neither recycle nor store.

BIBLIOGRAPHY

[1] Greer, A. L., “Metallic Glasses”, *Frontiers in Materials Science: Articles* 267, 1947-1957 (1995).

[2] http://en.wikipedia.org/wiki/Metallic_glass, “Amorphous metal – Wikipedia, the free encyclopedia”.

[3] Facchini, L. S., “Production and Characterization of Fe-based metallic glasses”, (2008).

[4] Pineda, E., “Vidres metàl·lics: viscositat i propietats elàstiques”, (2008).

[5] Ashby, M. F. and Greer, A. L., “Metallic glasses as structural materials”, *Scripta Materialia* 54, 321-326 (2006).

[6] Scopigno, T., Ruocco, G., Sette, F. and Monaco, G., “Is the Fragility of a Liquid Embedded in the Properties of Its Glass?”, *Science* 302, 849-852 (2003).

[7] Telford, M., “The case for bulk metallic glass”, *Materials Today*, 36-43 (2004).

[8] Serrano, J., Pineda, E., Bruna, P., Labrador, A., Le Tacone, M., Krische, M., Monaco, G., Wang, W.H. and Crespo, D., “Mechanical Properties of Bulk Metallic Glasses by Inelastic X-ray Scattering”, no published (2008).

[9] Luque, I. H., “Producció d’aliatges lleugers mitjançant solidificació ràpida”, (2007).

[10] Zhang, B., Pan, M.X., Zhao, D.Q. and Wang, W.H., “”Soft” bulk metallic glasses based on cerium”, *Applied Physics Letters* 85(1), 61-63 (2004).

[11] http://mse.iastate.edu/microscopy/home.html, “Scanning Electron Microscopy”.

[12] http://www.webelements.com, “WebElements Periodic Table of the Elements”.

[13] Compley, J. R. D. and Udovic, T. J., “Neutron Time-of-Flight Spectroscopy”, *J. Res. Natl. Inst. Stand. Technol*. 98 (1), 71-87 (1993).

[14] Rufflé, B., Parshin, D. A., Courtens, E. and Vacher, R., “Boson Peak and its Relation to Acoustic Attenuation in Glasses”, *Physical Review Letters* 100, 015501 (2008).

[15] http://www.tainstruments.com/product.aspx?id=25&n=1&siteid=11, “Q800”.

[16] Hachenberg, J. and Samwer, K., “Indications for a slow β-relaxation in a fragile metallic glass”, *Journal of Non-Crystalline Solids* 352, 5110-5113 (2006).

[17] Ferrer, M. L., Sakai, H., Kivelson, D. and Simionesco, C. A., “Extension of the Angell Fragility Concept”, *J. Phys. Chem. B* 103(20), 4191-4196 (1999).